

Measurement of the W -boson mass with the ATLAS detector

Andrés Pinto

05/12/2024



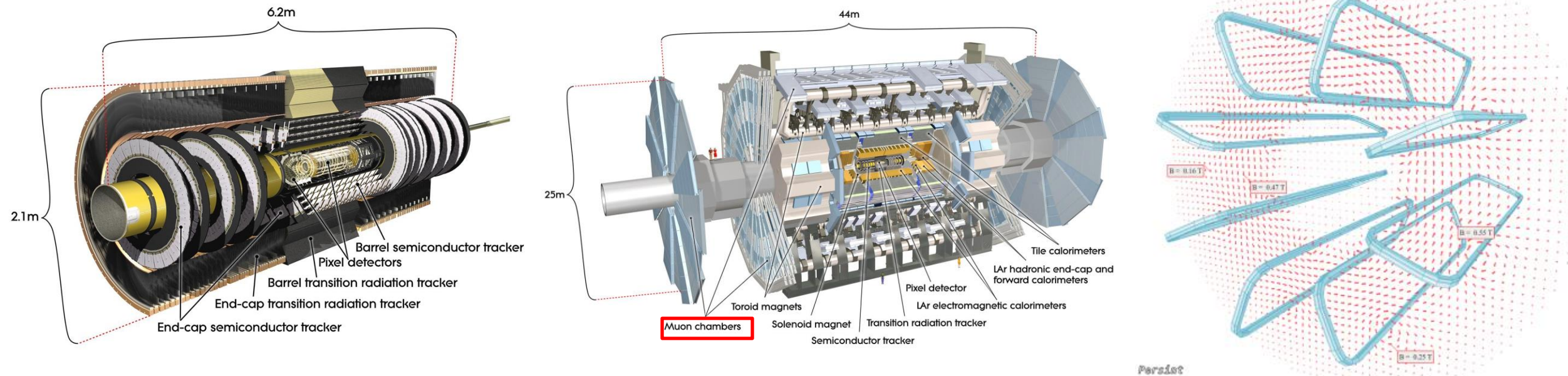
The Standard Model (SM) of particle physics

	mass →	$\approx 2.3 \text{ MeV}/c^2$	$\approx 1.275 \text{ GeV}/c^2$	$\approx 173.07 \text{ GeV}/c^2$	0	$\approx 126 \text{ GeV}/c^2$
	charge →	2/3	2/3	2/3	0	0
	spin →	1/2	1/2	1/2	1	0
		u up	c charm	t top	g gluon	H Higgs boson
QUARKS		$\approx 4.8 \text{ MeV}/c^2$	$\approx 95 \text{ MeV}/c^2$	$\approx 4.18 \text{ GeV}/c^2$	0	
		-1/3	-1/3	-1/3	0	
		1/2	1/2	1/2	1	
		d down	s strange	b bottom	γ photon	
		$0.511 \text{ MeV}/c^2$	$105.7 \text{ MeV}/c^2$	$1.777 \text{ GeV}/c^2$	$91.2 \text{ GeV}/c^2$	
		-1	-1	-1	0	
		1/2	1/2	1/2	1	
		e electron	μ muon	τ tau	Z Z boson	
LEPTONS		$< 2.2 \text{ eV}/c^2$	$< 0.17 \text{ MeV}/c^2$	$< 15.5 \text{ MeV}/c^2$	$80.4 \text{ GeV}/c^2$	
		0	0	0	± 1	
		1/2	1/2	1/2	1	
		ν_e electron neutrino	ν_μ muon neutrino	ν_τ tau neutrino	W W boson	
						GAUGE BOSONS

- Describes strong and Electroweak interactions.
- Explains the electroweak symmetry breaking via the Brout-Englert-Higgs mechanism.
- Particles:
 - Fermions: quarks and leptons.
 - Gauge bosons: gluon (g), photon (γ), W^\pm and Z
 - Scalar boson: Higgs boson (H)

The ATLAS detector

- Multi-purpose particle detector designed to study fundamental physics.
- **Sub-detectors:** Inner Detector (ID), calorimeters, Muon Spectrometer (MS), and a complex magnetic field.



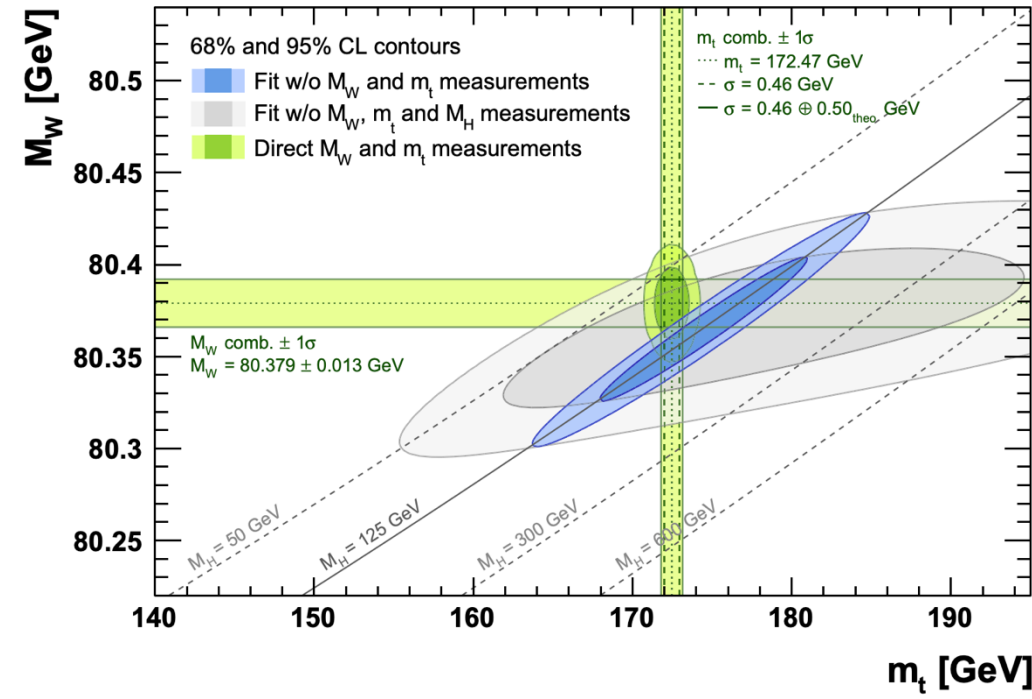
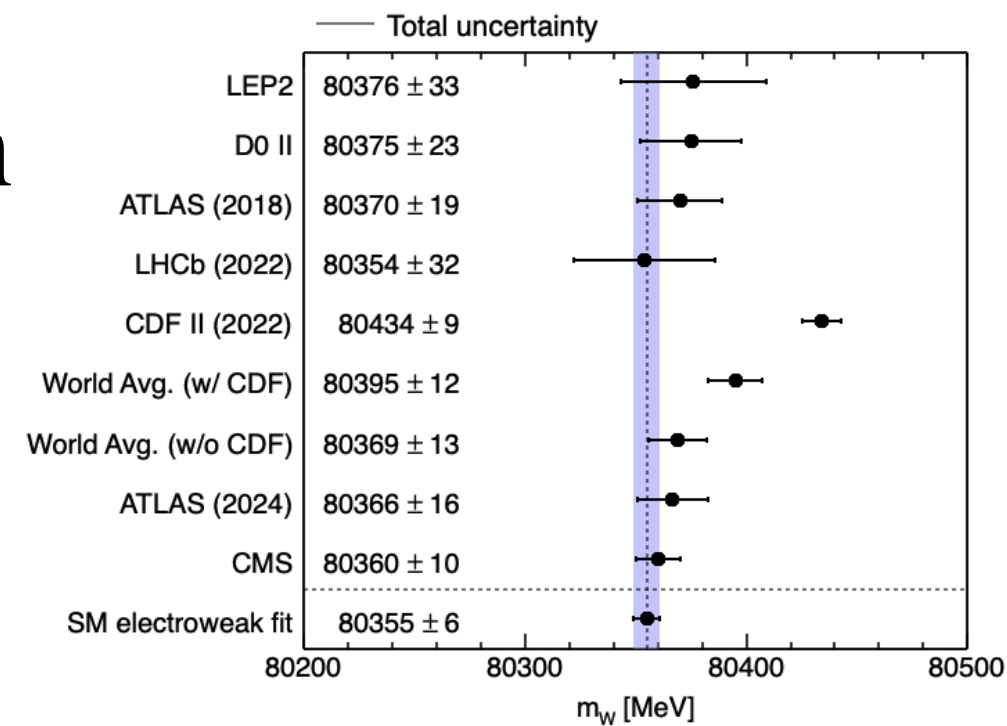
- **Muon system** is crucial for triggering and precise measurements, e.g. $pp \rightarrow W \rightarrow \mu\nu$.

4

Why measuring the W boson mass?

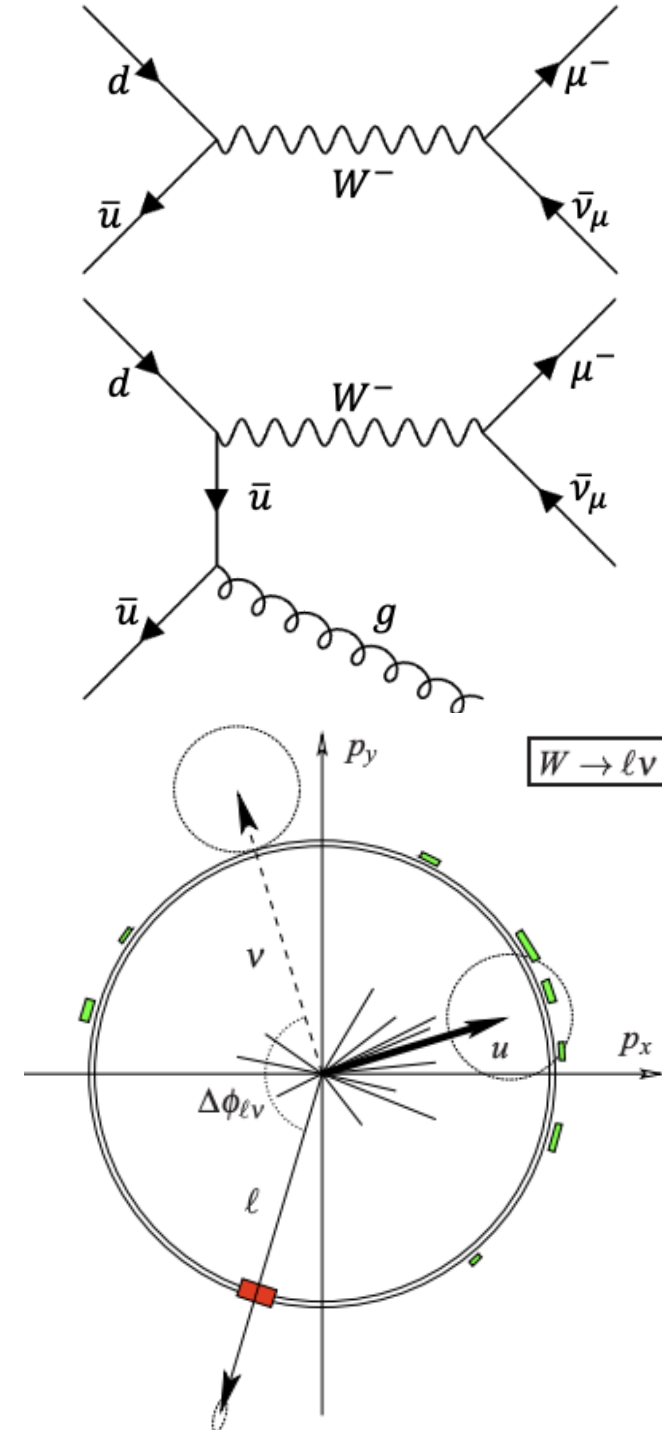
- The W boson mass (m_W) is important for testing the SM and BSM physics
- BSM scenarios could modify m_W by radiative corrections Δr .
- In the SM, these corrections come mainly from the top-quark and Higgs boson

$$m_W^2 \left(1 - \frac{m_W^2}{m_Z^2} \right) = \frac{\pi\alpha}{\sqrt{2} G_F} (1 + \Delta r)$$



W boson production and leptonic decay

- In the SM, the W boson can decay in quarks and leptons and its mass is measured in the lepton channels: $W \rightarrow \ell\nu$ ($\ell = e^\pm, \mu^\pm$).
- Higher-order corrections lead to a non-trivial p_T^W distribution that is crucial to control.
- This channel is challenging since the neutrino escapes the detection, and its momentum has to be inferred from other quantities.
- In the detector we measure:
 - The momentum of the charged lepton, p_T^ℓ .
 - The hadronic recoil, u_T .
- We can infer:
 - The energy of the neutrino: E_T^{miss}
 - The transverse mass: m_T



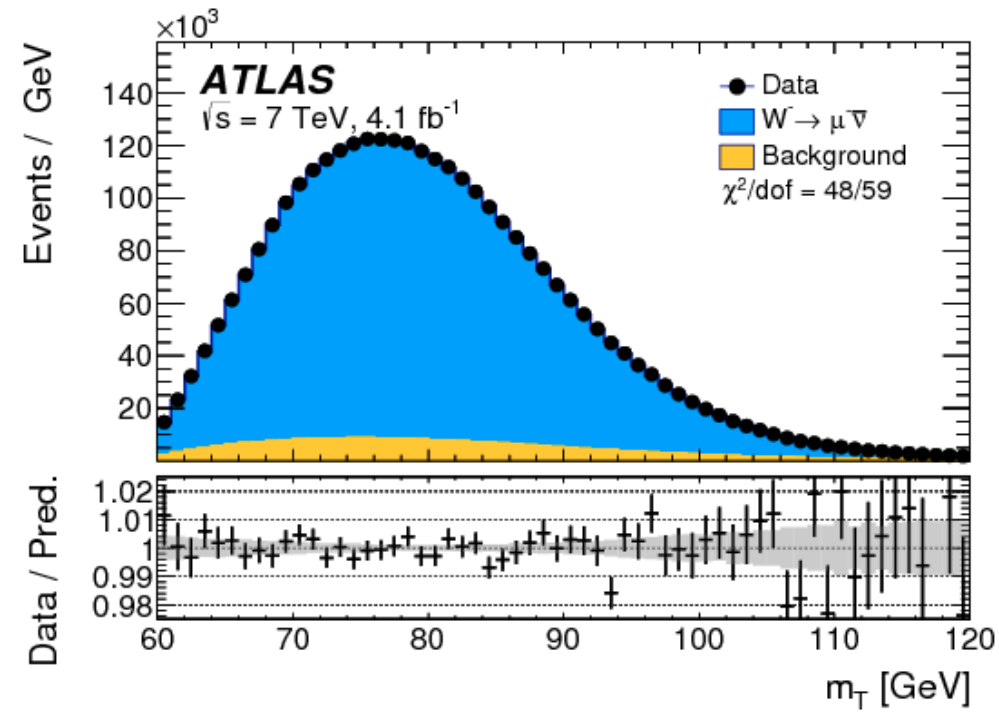
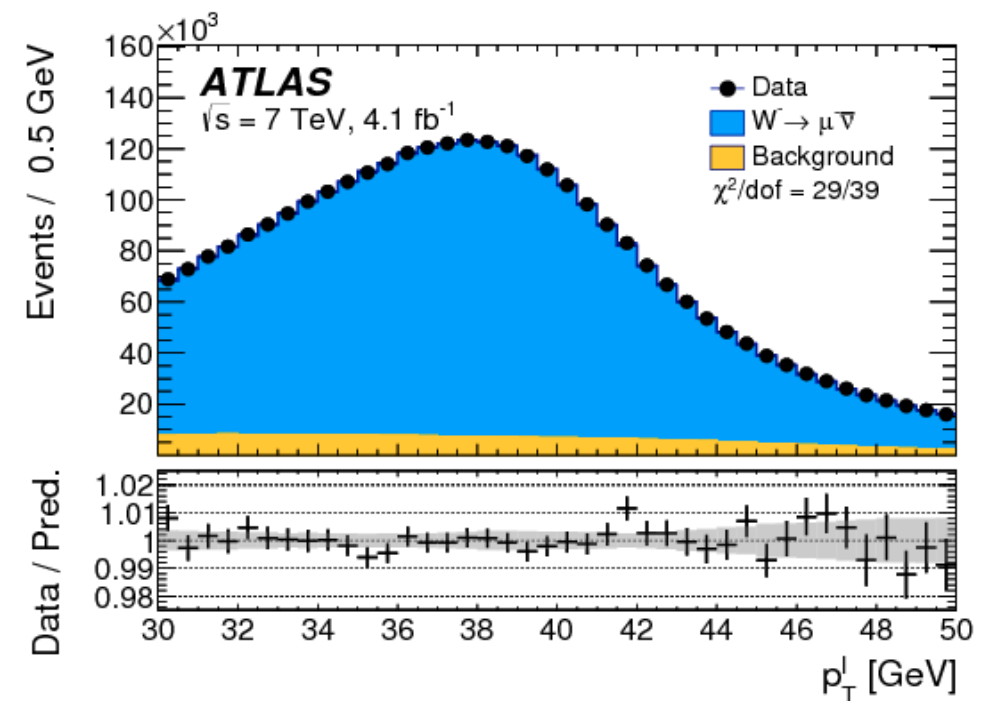
6

What do we measure?

- Observables sensitive to m_W
 - Lepton transverse momentum: p_T^ℓ
 - Transverse mass m_T

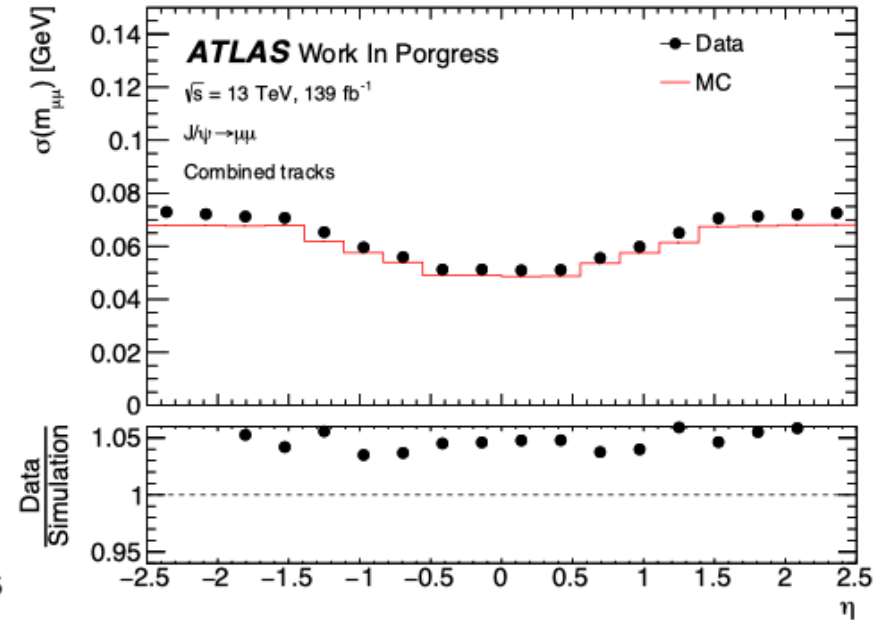
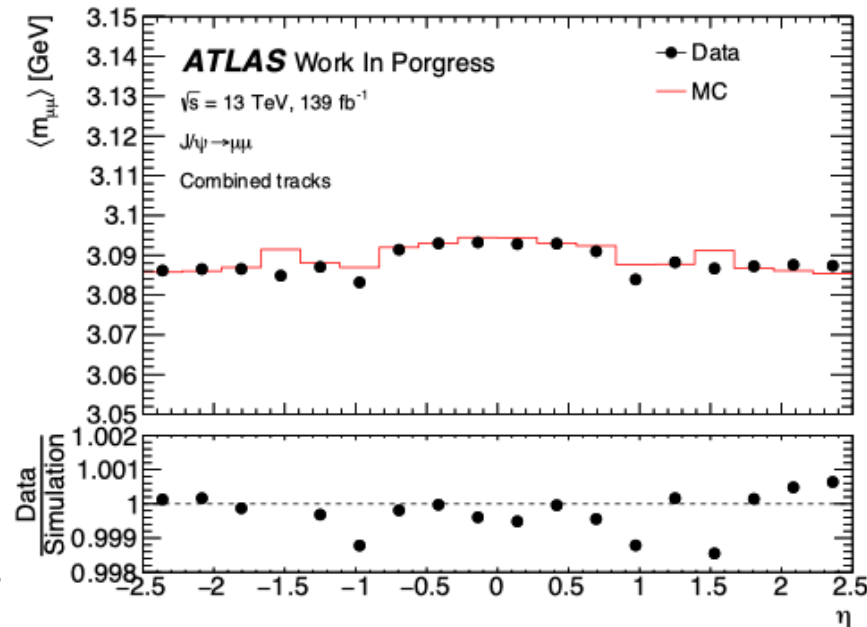
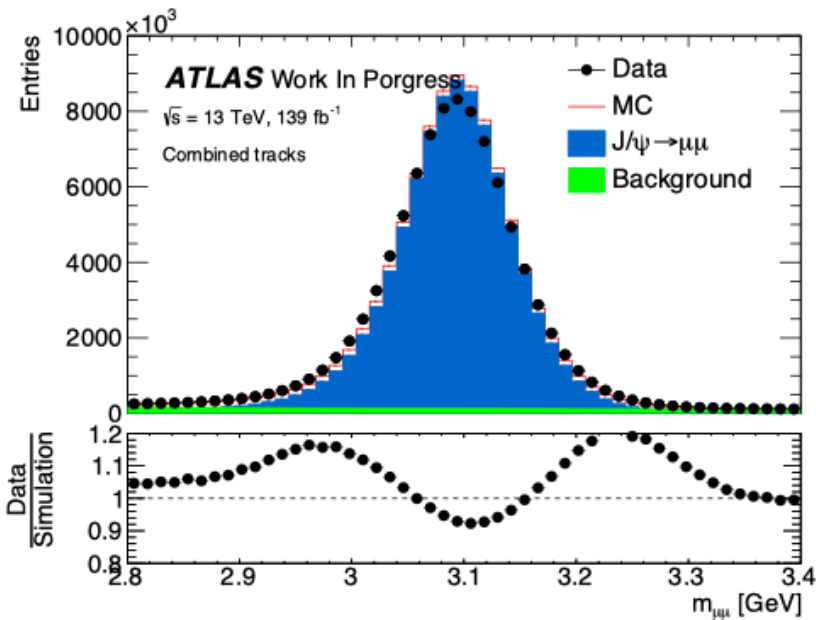
$$m_T = \sqrt{2p_T^\ell E_T^{miss} (1 - \cos\Delta\phi_{\ell\nu})}$$

- For p_T^ℓ , a good lepton calibration is required.
- For m_T , a precise calibration of u_T is required.
- My work is focused on:
 - Muon momentum calibration
 - Parameter estimation and uncertainty components



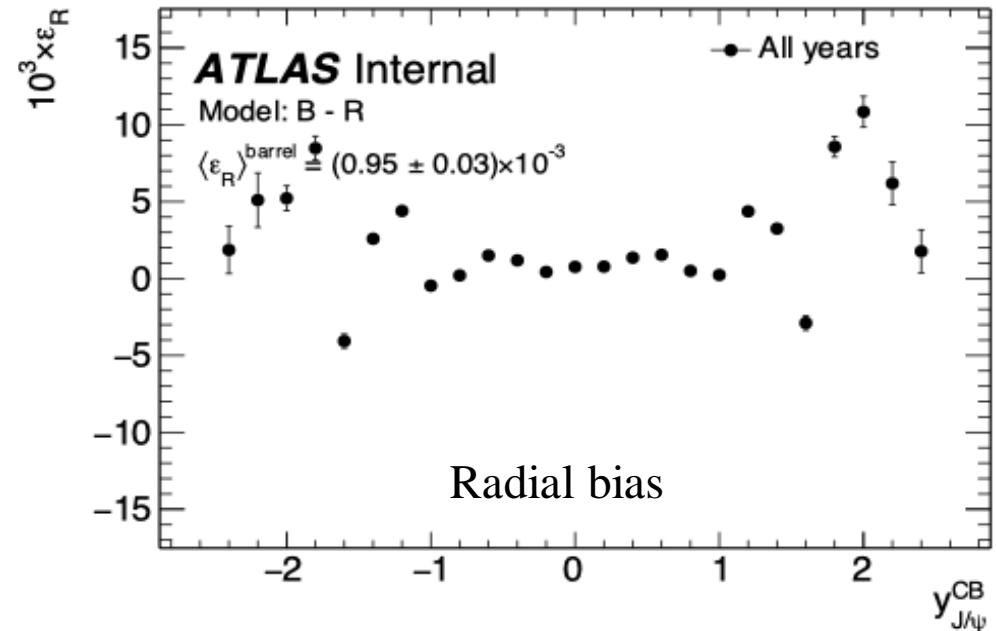
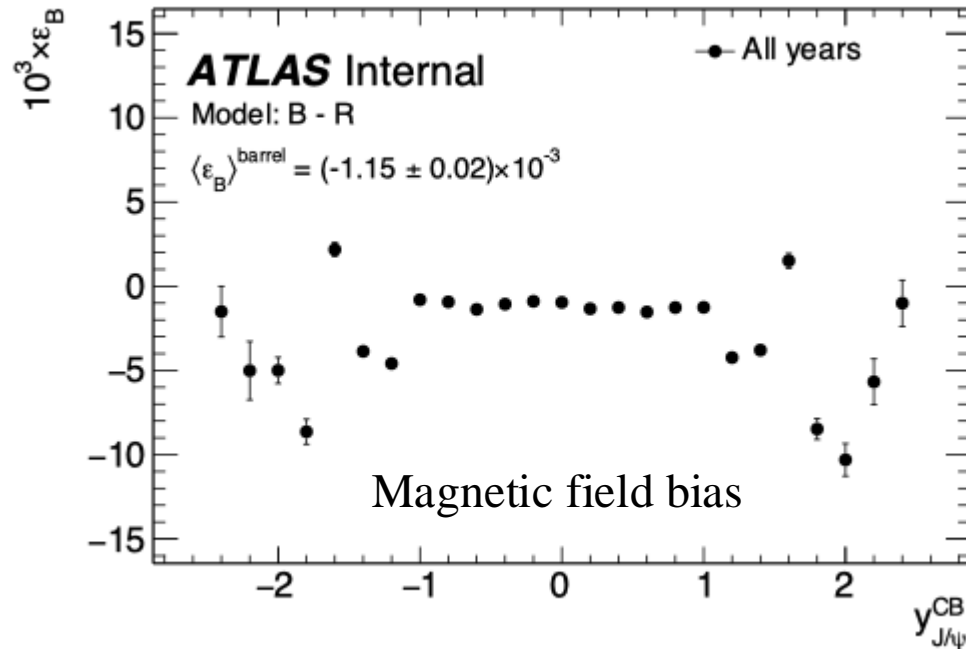
Detector calibration

- Muons are reconstructed in the MS and ID. A combined (CB) candidate is formed using the MS + ID.
- Different sources can affect the momentum of the muons in the detector, known as:
 - Sagitta bias
 - Inner tracker detector deformations (length-scale bias)
 - Magnetic field and resolution mismodelling
- Before calibration, data and simulation are not in good agreement.



Length-scale bias

- To look for ID distortions, we can use the $J/\psi \rightarrow \mu\mu$ resonance in a frame defined in J/ψ direction of flight.
- The invariant mass versus the azimuthal angle scan can provide hints of possible ID deformations in rapidity
- These deformations are modelled using magnetic field distortions and radial distortions
- **Final fits show an average bias of about $\langle \epsilon \rangle \sim 10^{-3}$**
- These maps are used to correct the data



Magnetic field and resolution mismodelling

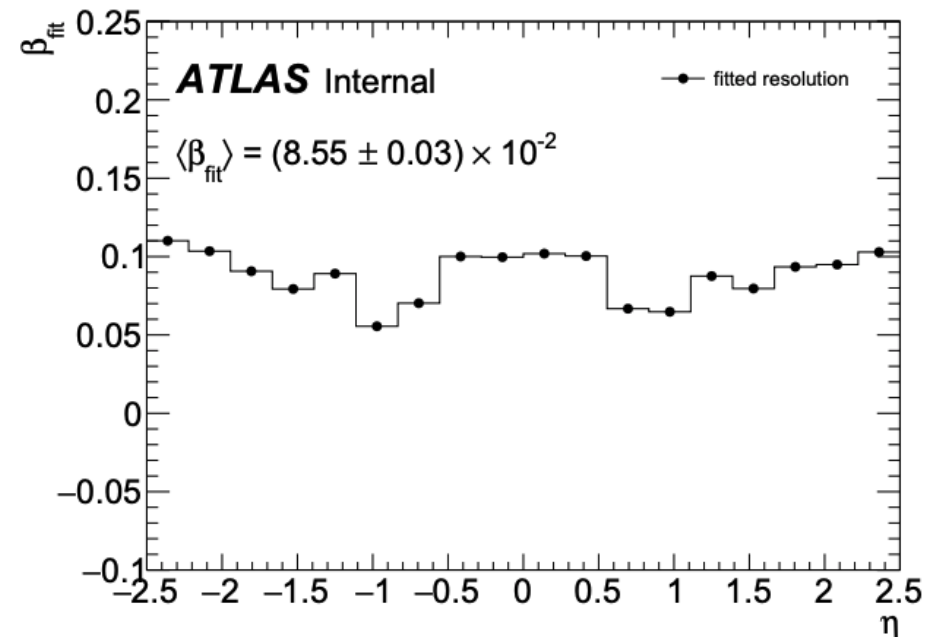
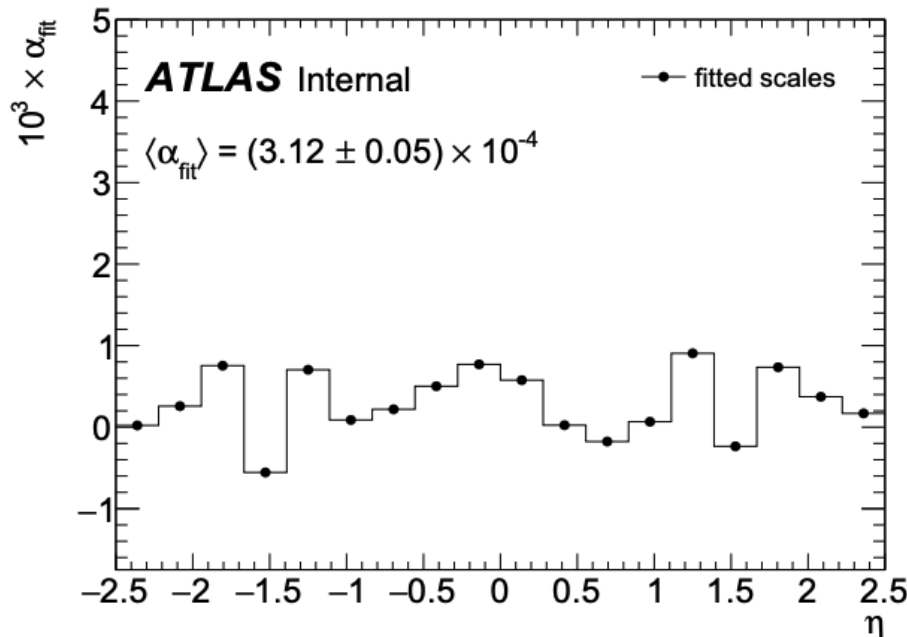
- After correcting for Sagitta and ID deformations, the next step is to correct for scale and resolution effects.
- The scale effect is modelled as a shift in the transverse momentum,

$$p_T^{scale} = (1 + \alpha) \cdot p_T^{reco}$$

- The resolution is modelled by smearing the di-muon invariant mass

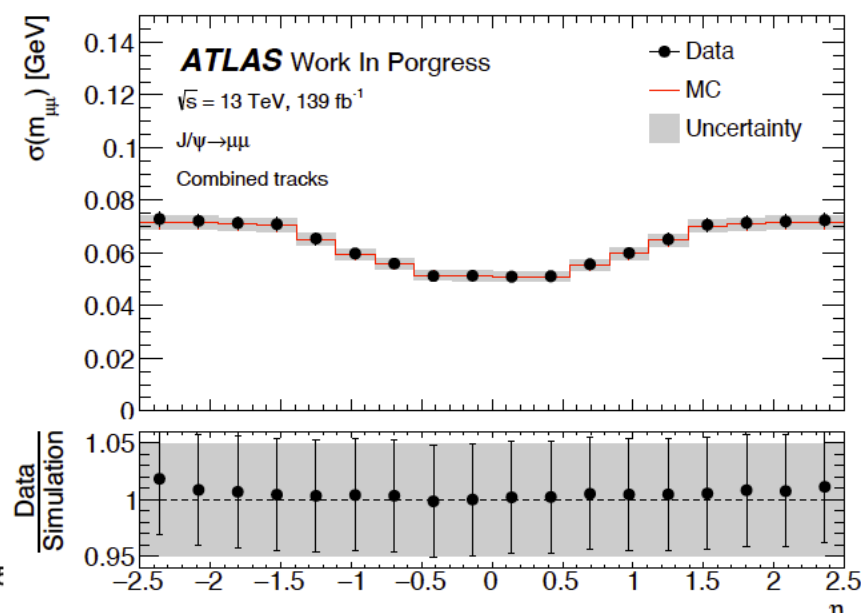
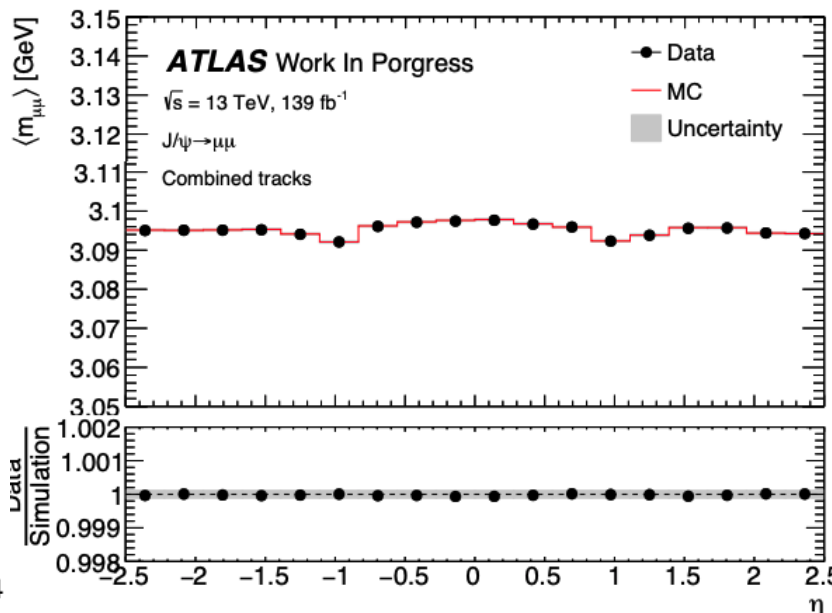
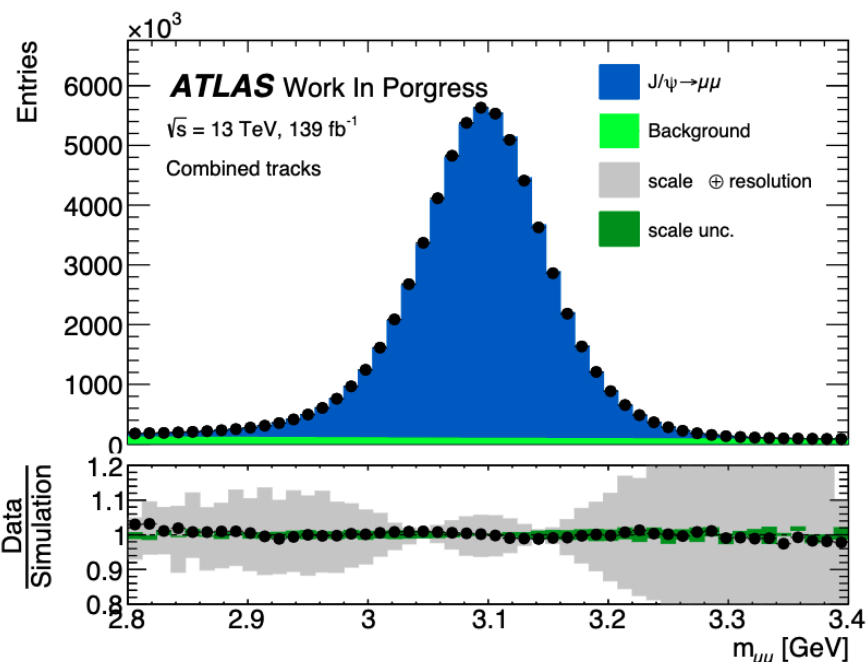
$$m_{\mu\mu}^{smear} = m_{\mu\mu}^{true} + (1 + \beta) \cdot (m_{\mu\mu}^{reco} - m_{\mu\mu}^{true})$$

- Templates are done to perform a fit of the invariant mass and to map the scale and resolution coefficients of the muons.



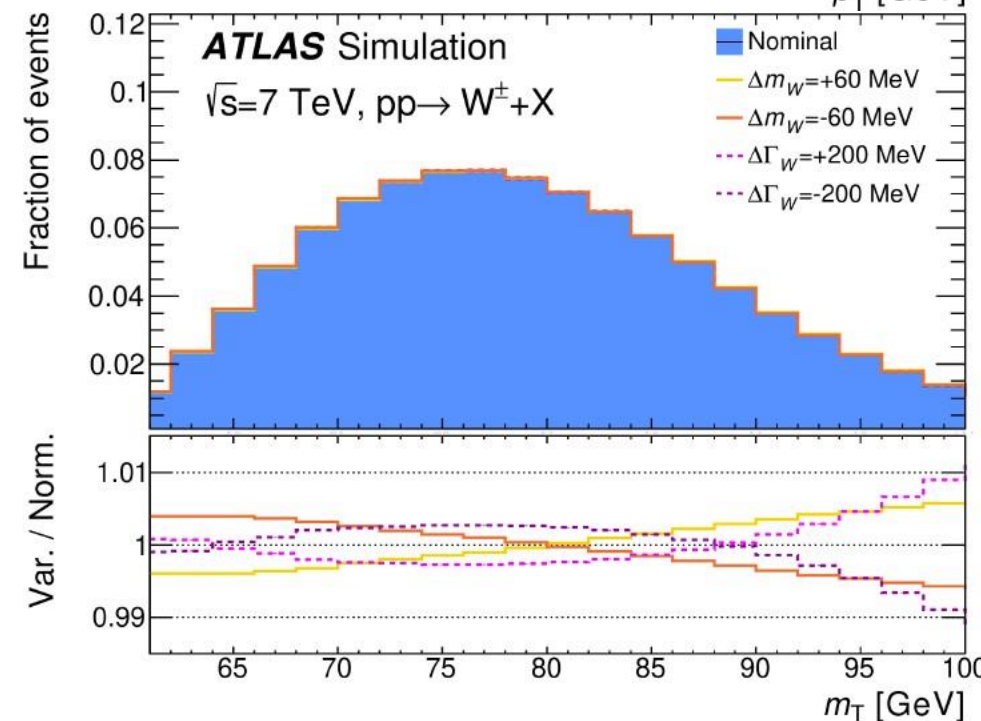
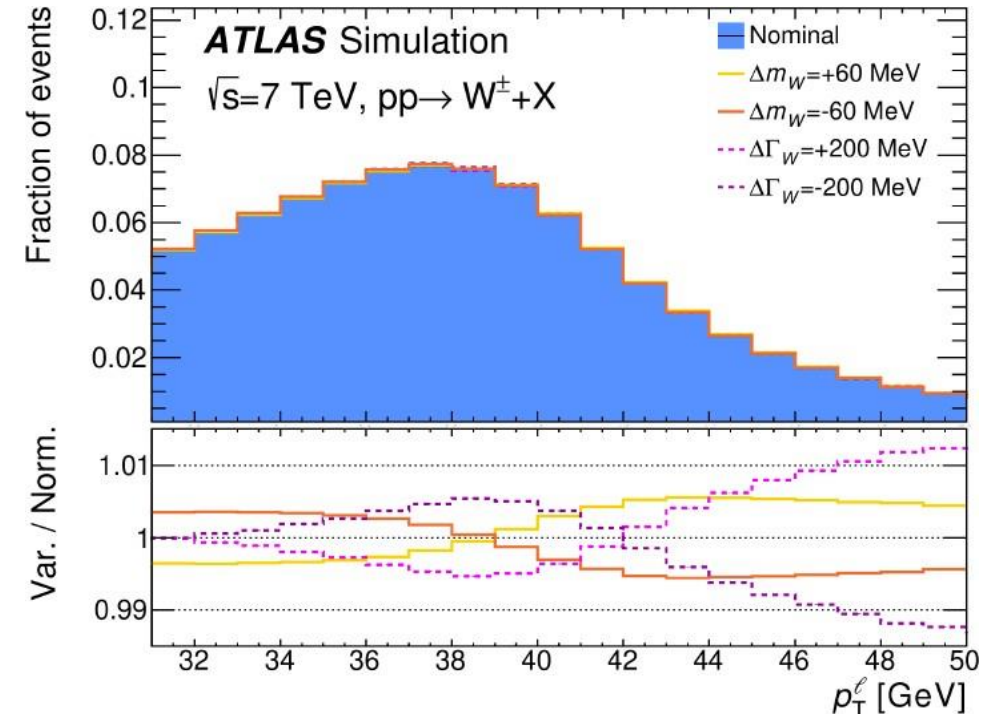
Final Muon Momentum Calibration

- After correction, a data-to-simulation agreement at the per mille level within the uncertainties is obtained. Systematics are evaluated by mass window variation.
- Relative systematic uncertainties of 8×10^{-5} in scale and 4×10^{-2} in resolution were found. **This is, a precision of about 6 MeV for m_W .**



How to measure the W boson mass?

- Once the calibration is done, we can use the corrected simulation to perform a fit data-to-simulation of W boson distributions.
- To extract m_W the template fit method is used.
- Different templates are done for different values of m_W .
- A likelihood function is maximized in order to find the template that best describes the data.
- At 7 TeV, two observables were used p_T^ℓ and m_T



Profile Likelihood fit for W mass

- The likelihood is given by,

$$\mathcal{L}(\vec{m}|\vec{\theta}, \vec{\alpha}) = \prod_i \text{Poisson}(m_i|\nu_i(\vec{\theta}, \vec{\alpha})) \cdot \prod_r \text{Gauss}(\alpha_r|a_r)$$

Poisson likelihood for each bin

Constraint terms for the nuisance parameters: Systematics are assumed to be Gaussian distributed.

- m_i : Observed data per bin
- $\vec{\theta}$: POI (m_W)
- $\vec{\alpha}$: NP for systematics
- \vec{a} : Global observable for nuisance parameter.
- ν_i : Total prediction per bin \rightarrow

$$\begin{aligned} \nu_{ji}(\vec{\theta}, \vec{\alpha}) = & \Phi \times \left[S_{ji}^{\text{nom}} + \sum_p \theta_p \times (S_{ji}^{\theta_p} - S_{ji}^{\text{nom}}) \right] \\ & + \sum_s \alpha_s \times (S_{ji}^s - S_{ji}^{\text{nom}}) \\ & + B_{ji}^{\text{nom}} + \sum_b \alpha_b \times (B_{ji}^b - B_{ji}^{\text{nom}}), \end{aligned}$$

Φ : normalization factor.

S : signal

B : background

Profile Likelihood fit for W mass

- In the Gaussian limit, the likelihood admits an analytical solution ([Eur. Phys. J. C, vol. 84, 2024](#)) that allows to simplify the calculations:

$$\begin{aligned}
 -2 \ln \mathcal{L}(\vec{\theta}, \vec{\alpha}) &= \sum_{i,j} \left(m_i - t_i(\vec{\theta}) - \sum_r \Gamma_{ir}(\alpha_r - a_r) \right) V_{ij}^{-1} \left(m_j - t_j(\vec{\theta}) - \sum_s \Gamma_{js}(\alpha_s - a_s) \right) \\
 &\quad + \sum_r (\alpha_r - a_r)^2.
 \end{aligned}$$

- This approach is particularly useful to study the uncertainty components.
- The systematic components can be properly evaluated.
- This can be generalized to non-Gaussian limits through the global shifted observable method.

Uncertainty components

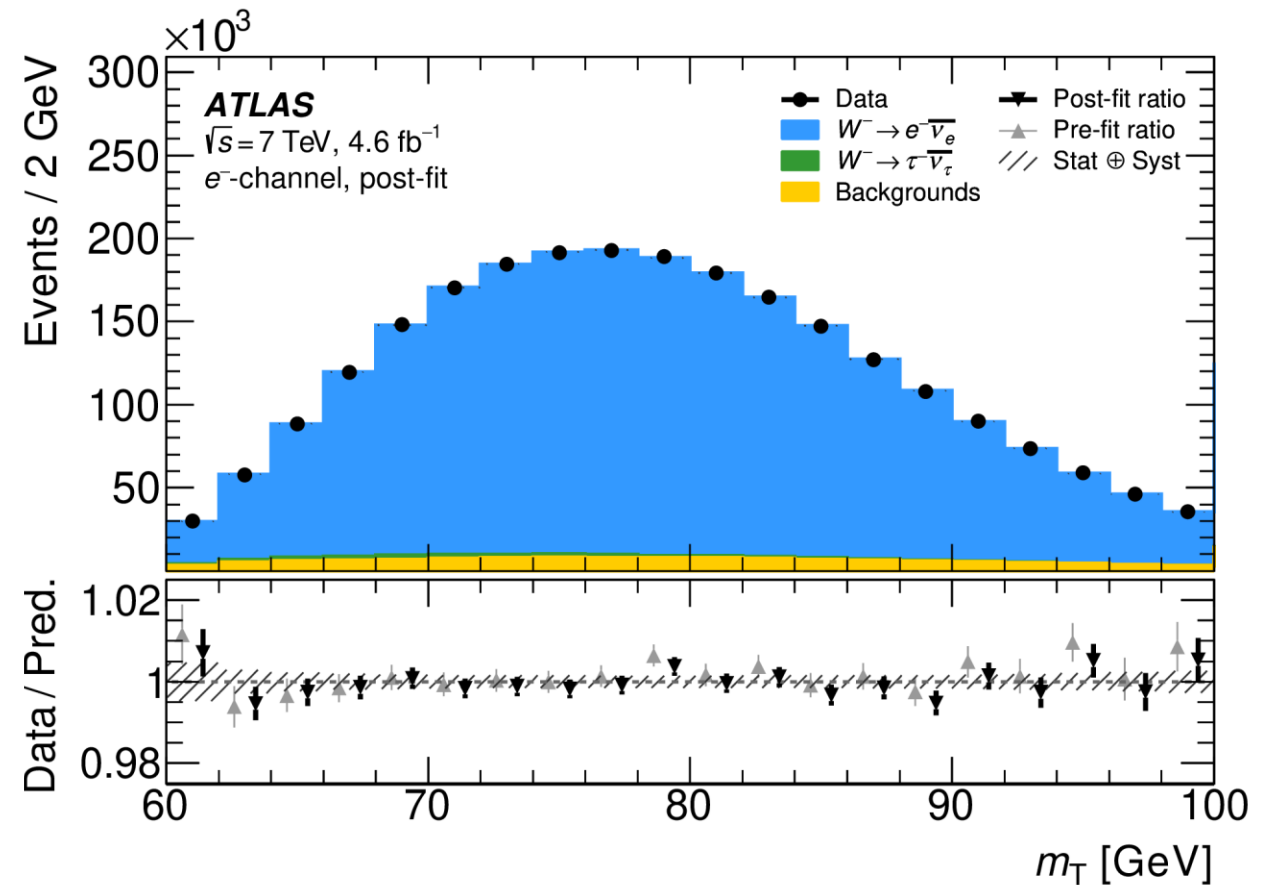
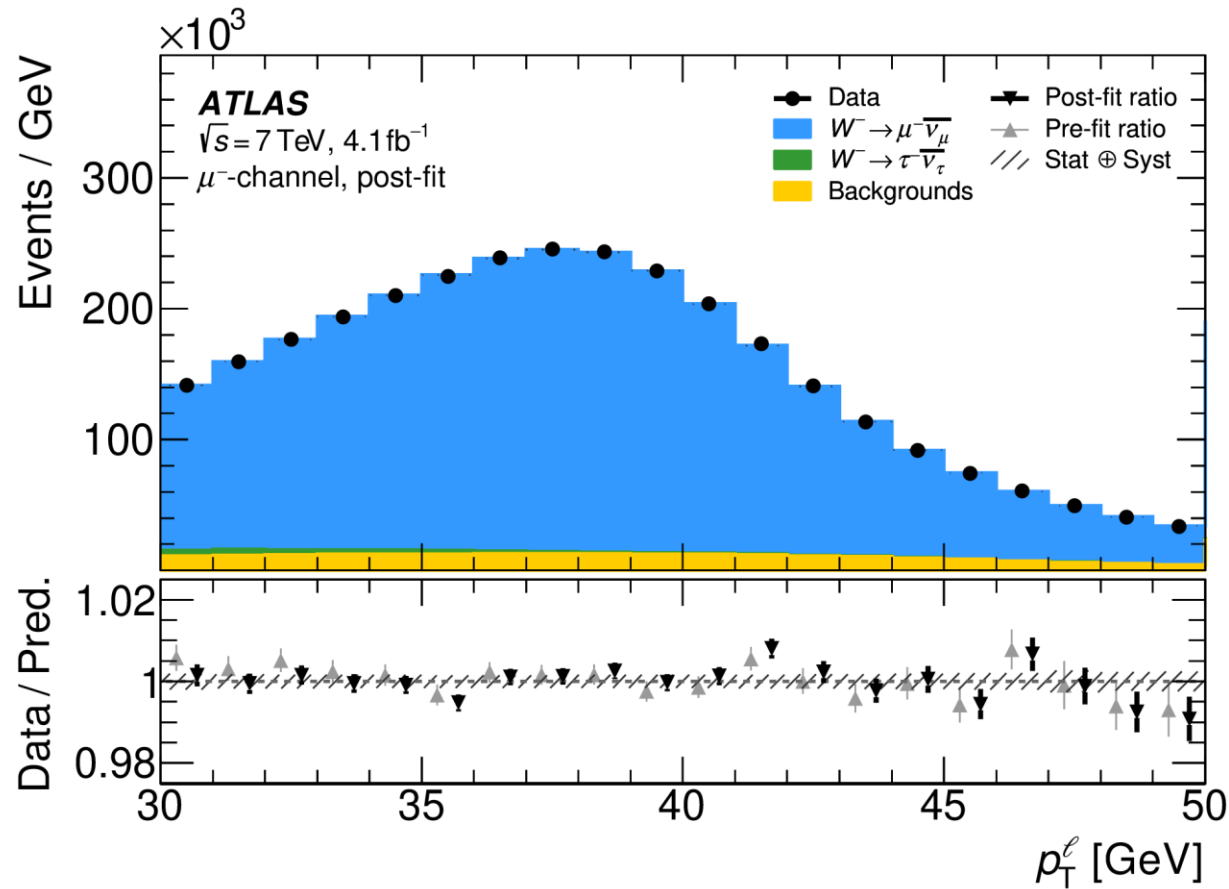
In the Gaussian limit, the likelihood covariance can be divided in three block matrices:

$$\begin{array}{c}
 \text{Nuisance parameters} \\
 \text{covariance matrix} \\
 \downarrow \\
 \text{cov}(-2 \ln \mathcal{L}) = \left(\begin{array}{c|c} \text{cov}(\hat{\alpha}_r, \hat{\alpha}_s) & \text{cov}(\hat{\alpha}_r, \hat{\theta}_q) \\ \hline \text{cov}(\hat{\theta}_p, \hat{\alpha}_s) & \text{cov}(\hat{\theta}_p, \hat{\theta}_q) \end{array} \right) \\
 \uparrow \qquad \qquad \qquad \uparrow \\
 \text{Systematic uncertainty} \quad \text{Parameter of interest} \\
 \text{components} \qquad \qquad \text{covariance matrix}
 \end{array}$$

$$\begin{aligned}
 \sigma_{\text{total}} &= \sqrt{\text{cov}(\hat{\theta}_p, \hat{\theta}_p)}, \\
 \sigma_{\text{syst}} &= \sqrt{\sum_r \text{cov}(\hat{\theta}_p, \hat{\alpha}_r) \text{cov}(\hat{\alpha}_r, \hat{\theta}_p)}, \\
 \sigma_{\text{stat}} &= \sqrt{\sigma_{\text{total}}^2 - \sigma_{\text{syst}}^2},
 \end{aligned}$$

Pre-fit and Post-fit plots

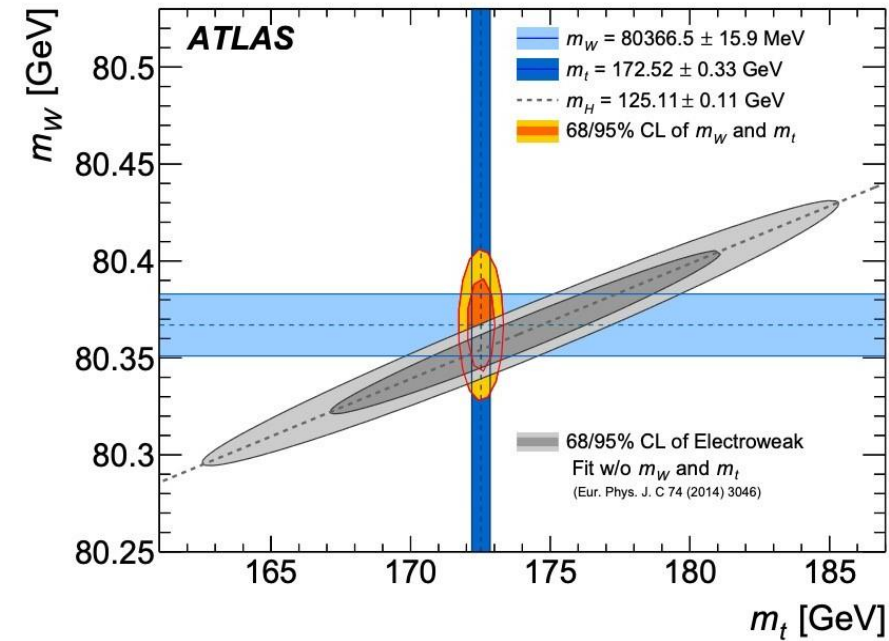
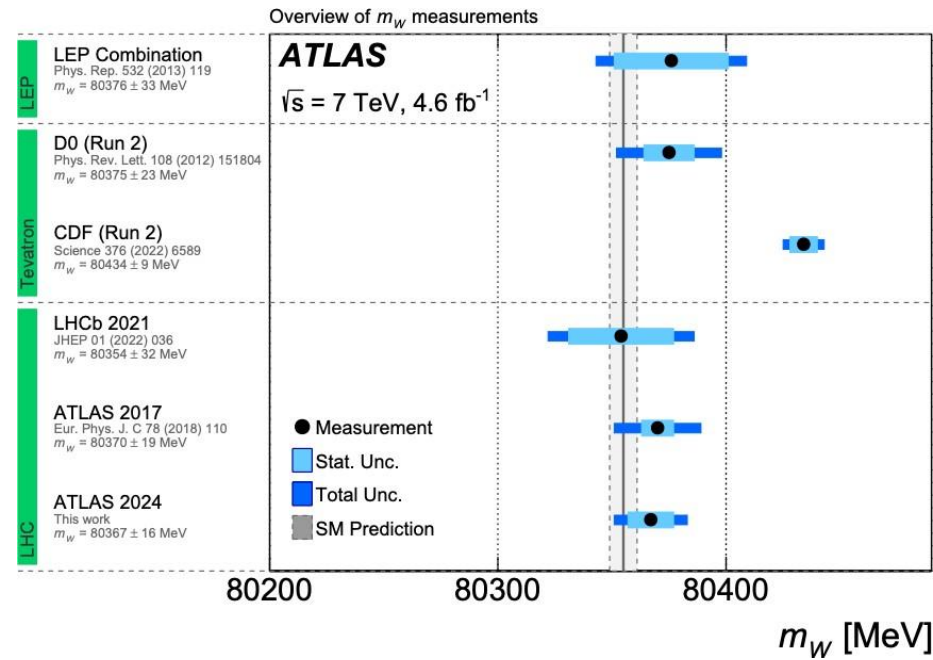
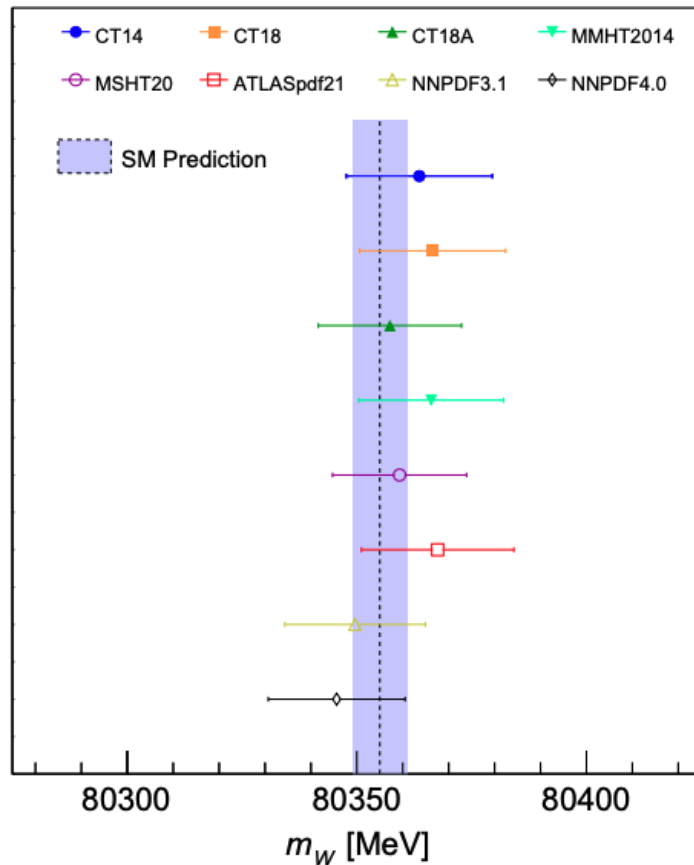
The post-fit, $|\eta|$ –inclusive p_T^ℓ , m_T distributions obtained with CT18 agree with the data within the uncertainties.



m_W measurement at $\sqrt{s} = 7$ TeV

- The final $p_T^\ell - m_T$ combination is performed using the BLUE approach where the correlation is obtained by pseudo-experiments. CT18 PDF set is chosen as baseline.
- Result agrees with the SM and improvement with respect to 2017 of about 15%.

([arXiv:2403.15085](https://arxiv.org/abs/2403.15085)).



m_W measurement at $\sqrt{s} = 7$ TeV

- Final result corresponds to,

$$m_W = 80366.5 \pm 15.9 (\pm 9.8 \pm 12.5) \text{ MeV}$$

- With uncertainty decomposition,

Unc. [MeV]	Total	Stat.	Syst.	PDF	A_i	Backg.	EW	e	μ	u_T	Lumi	Γ_W	PS
p_T^ℓ	16.2	11.1	11.8	4.9	3.5	1.7	5.6	5.9	5.4	0.9	1.1	0.1	1.5
m_T	24.4	11.4	21.6	11.7	4.7	4.1	4.9	6.7	6.0	11.4	2.5	0.2	7.0
Combined	15.9	9.8	12.5	5.7	3.7	2.0	5.4	6.0	5.4	2.3	1.3	0.1	2.3

- In 2017, PDF unc. was ~ 9 MeV and $A_i + p_T^W$ unc. was ~ 8 MeV which means an improvement of about 37% and 45% respectively

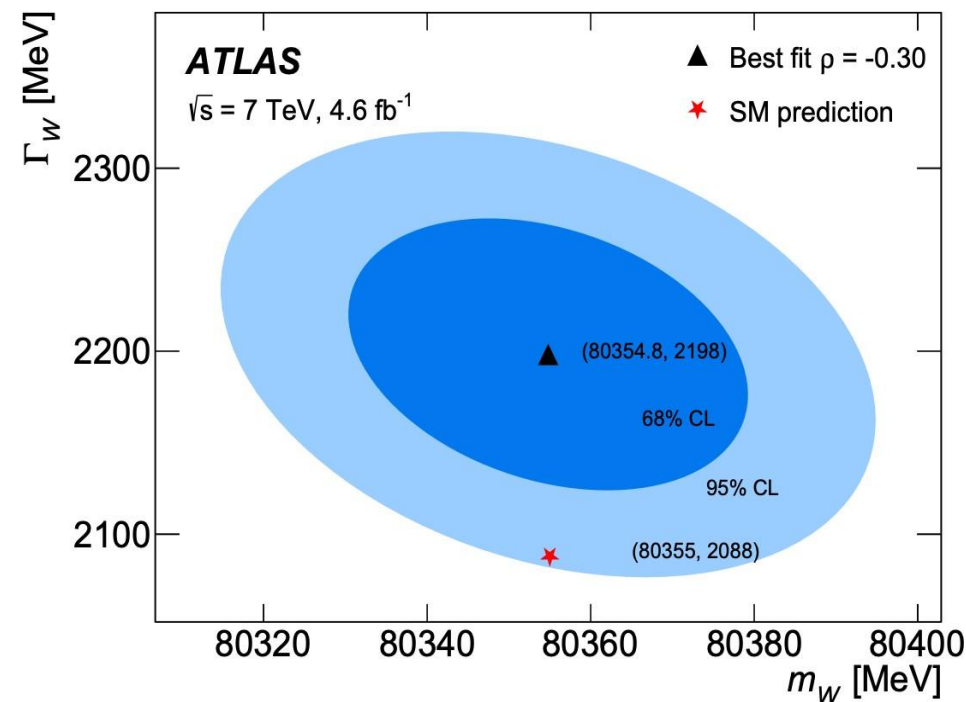
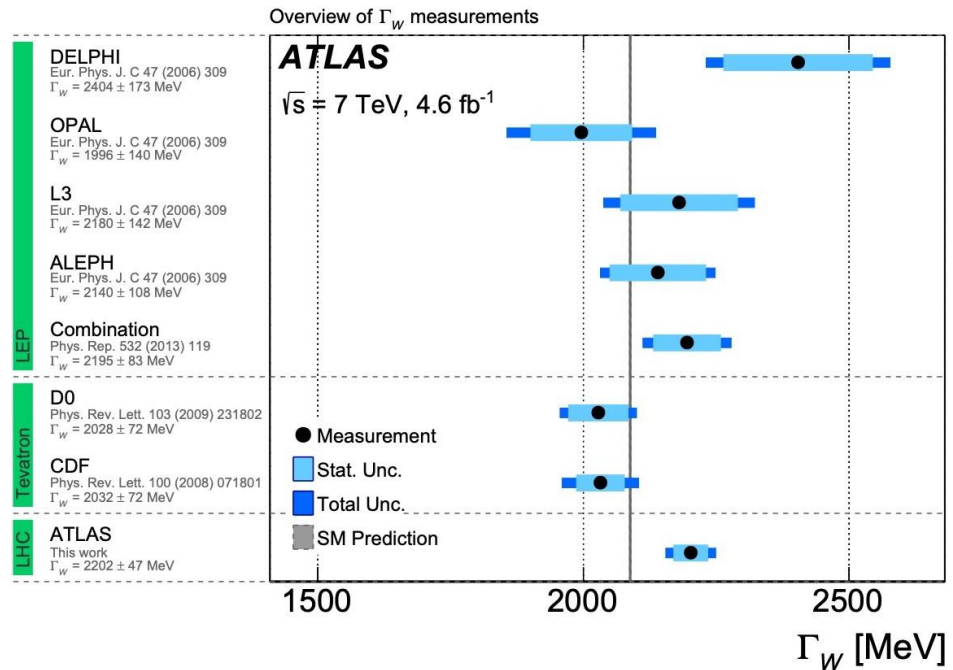
Measuring the W width at 7 TeV

- The W -boson width was measured in a similar strategy. This is so far, the most precise measurement of Γ_W .
- Result is consistent with the SM within 2 standard deviations.

$$\Gamma_W = 2202 \pm 47 (\pm 32 \pm 34) \text{ MeV}$$

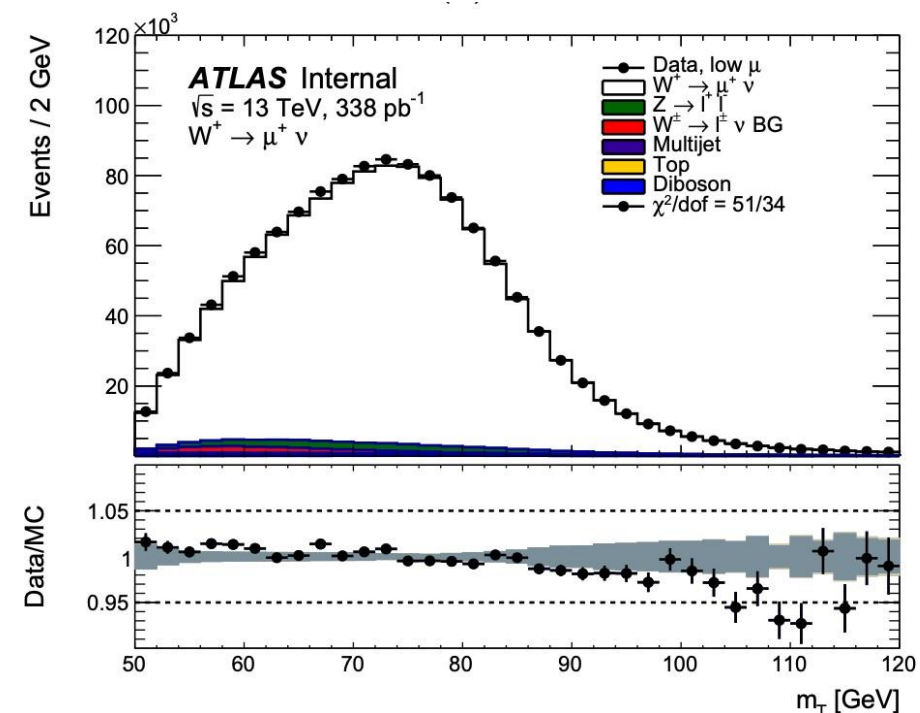
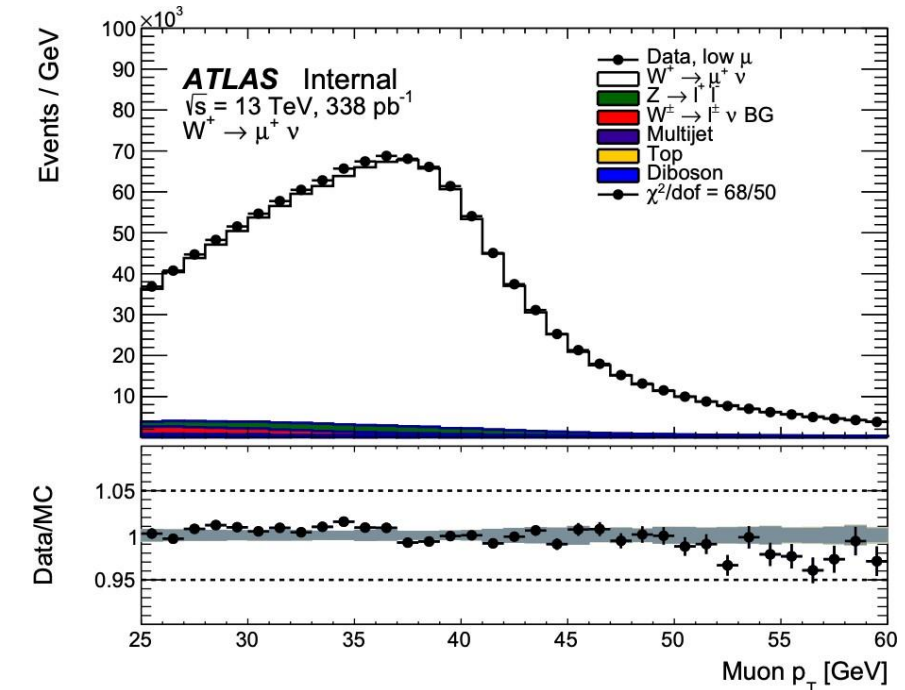
- With uncertainty decomposition:

Unc. [MeV]	Total	Stat.	Syst.	PDF	A_i	Backg.	EW	e	μ	u_T	Lumi	m_W	PS
p_T^ℓ	72	27	66	21	14	10	5	13	12	12	10	6	55
m_T	48	36	32	5	7	10	3	13	9	18	9	6	12
Combined	47	32	34	7	8	9	3	13	9	17	9	6	18



Current status in m_W

- Currently, the ATLAS collaboration prepares a new measurement of m_W using low pile-up data set at 5.02 TeV and 13 TeV.
- This dataset is of particular interest since it provides a better resolution in the transverse mass.
- This result in an increased sensitivity of m_T to m_W .
- These conditions provide a good modelling for the transverse momentum of the W boson, p_T^W , which is one of the large uncertainty sources in this measurement.
- Preliminary results show a competitive precision compared to other experiments.



Conclusions

- My work was focused on the W -boson mass measurement for which I developed the muon calibration and a fitting strategy for the uncertainty components.
- Muon calibration work chain shows a good performance with a data-to-simulation agreement at the per mille level.
- Profile likelihood fit improved the m_W and Γ_W precision with respect to 2017 measurement, leading to:

$$m_W = 80366.5 \pm 15.9 (\pm 9.8 \pm 12.5) \text{ MeV}$$

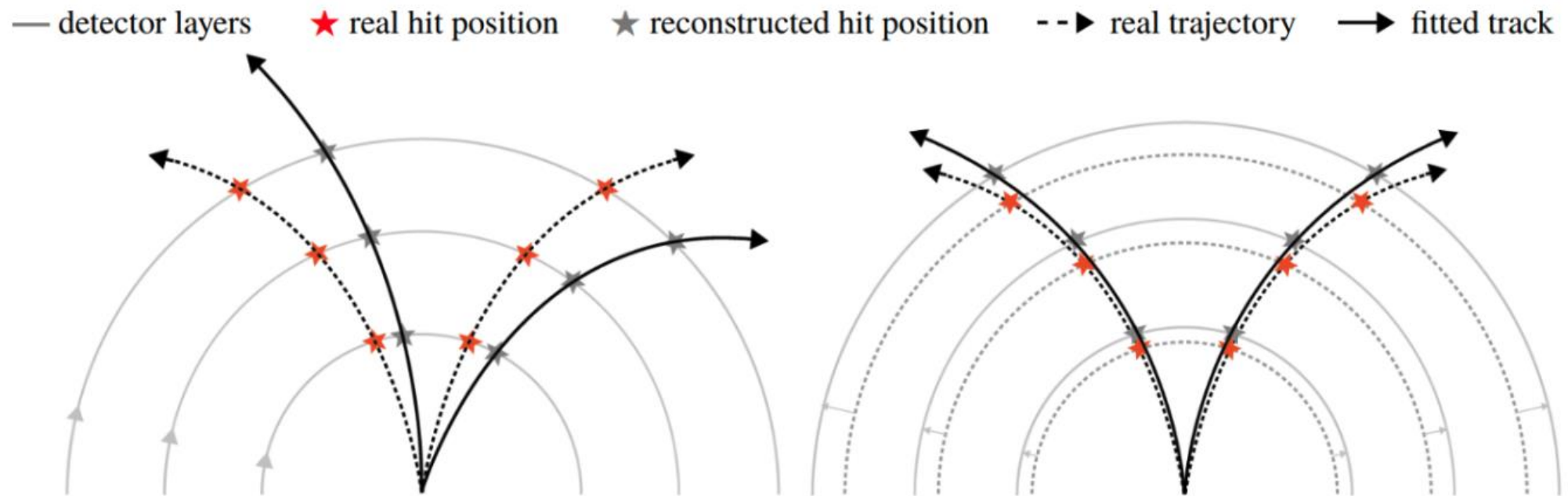
$$\Gamma_W = 2202 \pm 47 (\pm 32 \pm 34) \text{ MeV}$$

- New measurement of m_W using low pile-up dataset is in progress with preliminary results showing a competitive precision.

BACKUP

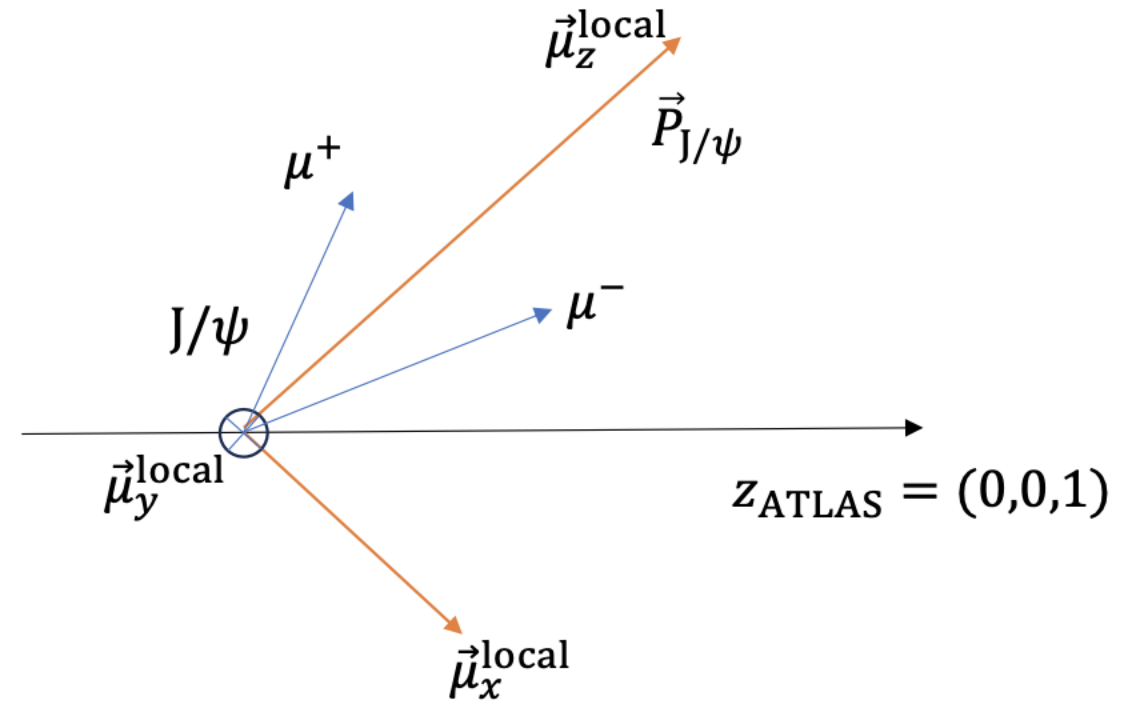
Tracking biases

- The two most common deformations that bias the curvature (momentum) are:
 - **Sagitta bias:** rotation of the detector layers (charge dependent).
 - **Length-scale bias:** radial expansion of the detector layers (charge independent).



Local frame

- Defined in the J/ψ momentum direction.
- This frame is not affected by a boost
- We defined only one angle: ϕ
- Templates are prepared to fit the data



$$\vec{\mu}_z^{\text{local}} = \frac{\vec{P}_{J/\psi}}{|\vec{P}_{J/\psi}|}$$

$$\vec{\mu}_x^{\text{local}} = \frac{\vec{\mu}_y^{\text{local}} \times \vec{\mu}_z^{\text{local}}}{|\vec{\mu}_y^{\text{local}} \times \vec{\mu}_z^{\text{local}}|}$$

$$\vec{\mu}_y^{\text{local}} = \frac{\vec{\mu}_z^{\text{local}} \times z_{\text{ATLAS}}}{|\vec{\mu}_z^{\text{local}} \times z_{\text{ATLAS}}|}$$

$$\phi_{\text{local}}^+ = \text{atan} \left(\frac{\vec{p}^+ \cdot \mu_y^{\text{local}}}{\vec{p}^+ \cdot \mu_x^{\text{local}}} \right)$$

ID deformation models

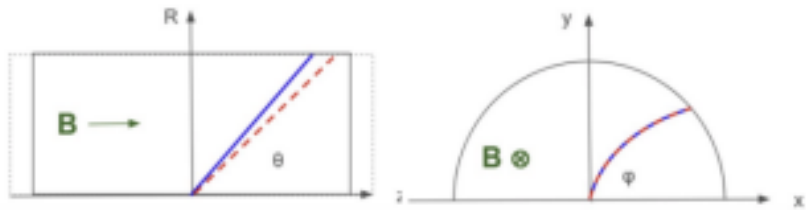
• Longitudinal (Z) model:

- Affects the **longitudinal** component of the momentum.

- $p'_T = p_T$

- $p'_z = (1 + \varepsilon_z) \cdot p_z$

- $\cot\theta' = (1 + \varepsilon_z) \cdot \cot\theta$



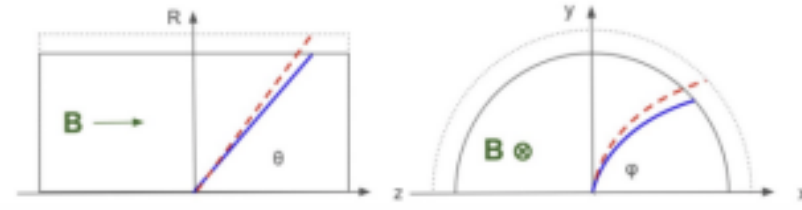
• Radial (R) model:

- Affects the **transverse** component of the momentum.

- $p'_T = (1 + \varepsilon_R) \cdot p_T$

- $p'_z = p_z$

- $\cot\theta' = \cot\theta / (1 + \varepsilon_R)$



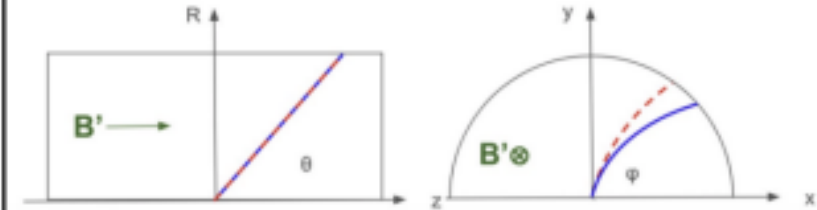
• Magnetic field (B) model:

- Affects both transverse and longitudinal component of the momentum.

- $p'_T = (1 + \varepsilon_B) \cdot p_T$

- $p'_z = (1 + \varepsilon_B) \cdot p_z$

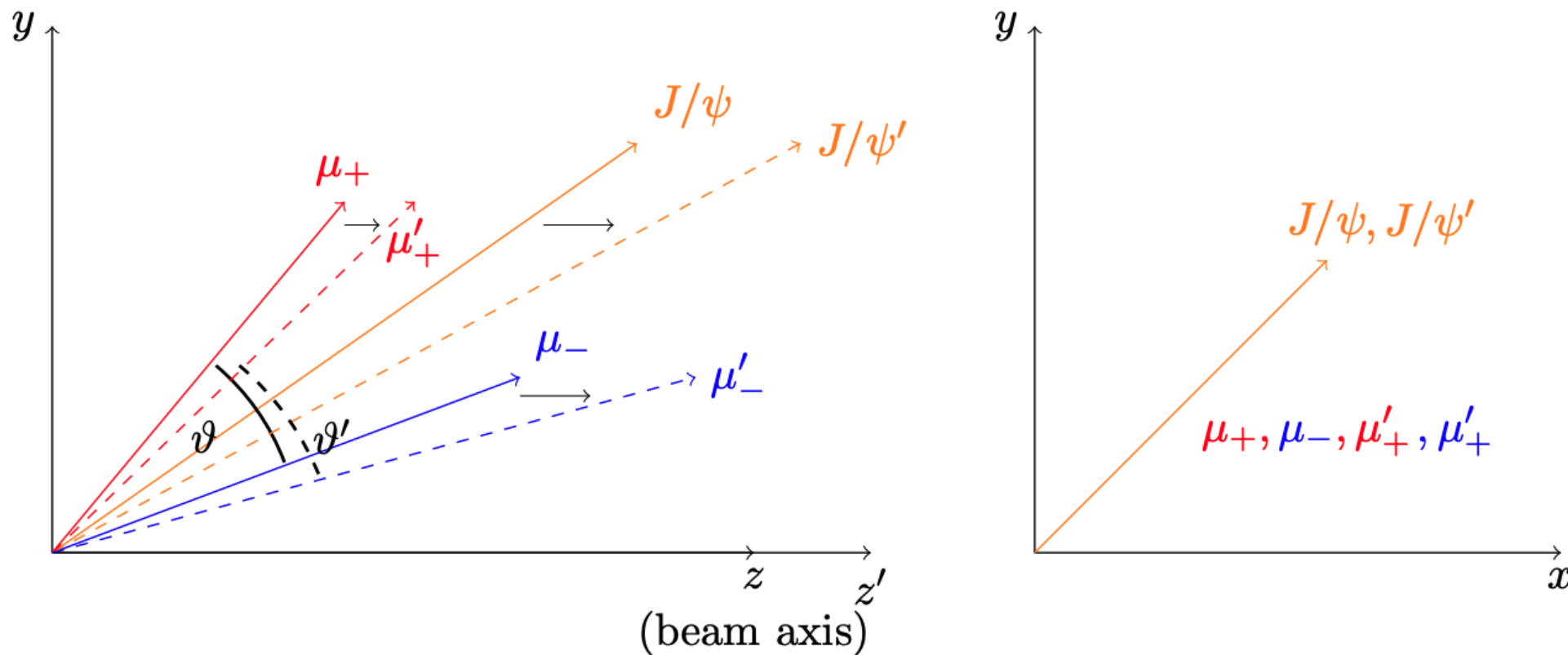
- $\cot\theta' = \cot\theta$



Length-scale bias

Detector deformations can be studied using the invariant mass in $J/\psi \rightarrow \mu\mu$ decay.
Both muons at same φ and different pseudo-rapidity η .

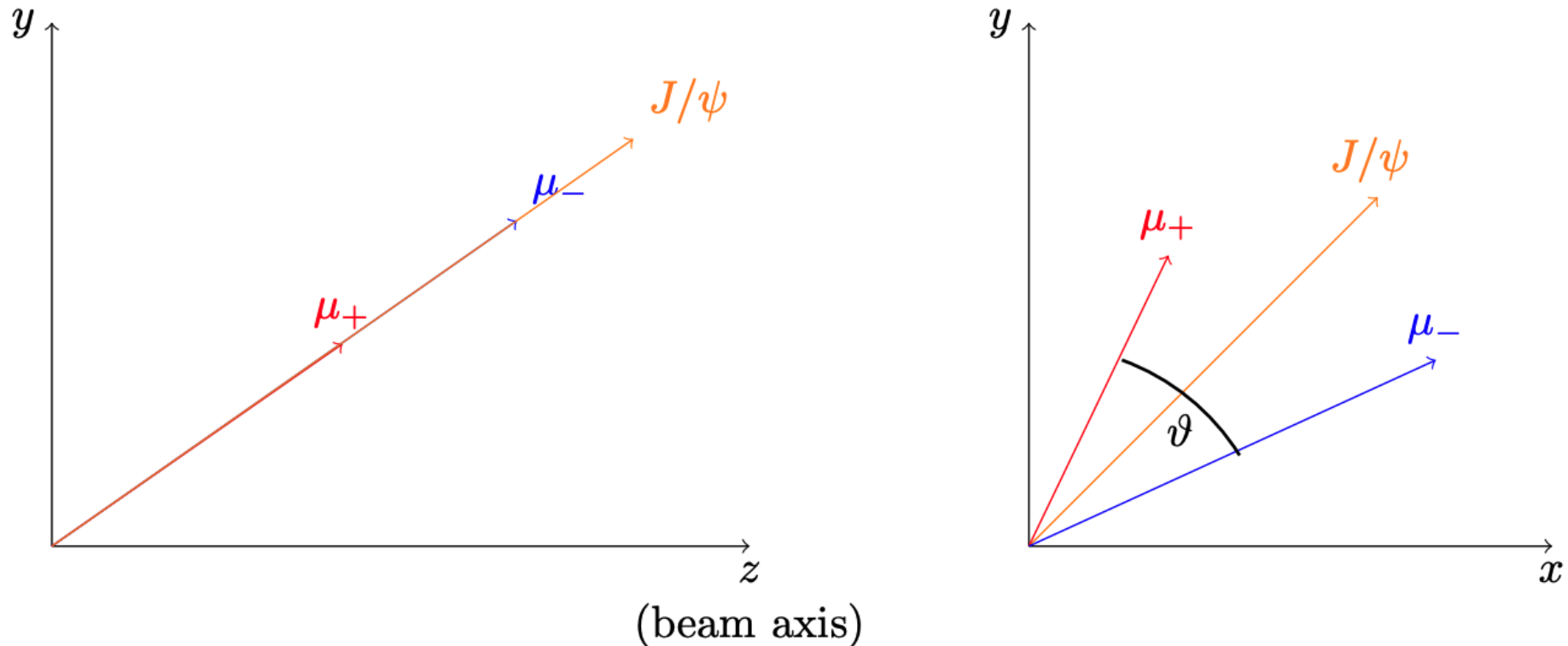
$$m_{\mu\mu}^2 \propto (1 - \cos \vartheta) \implies m_{\mu\mu}^{2,\prime} \propto (1 - \cos \vartheta')$$



Length-scale bias

Both muons at different φ and same pseudo-rapidity η .

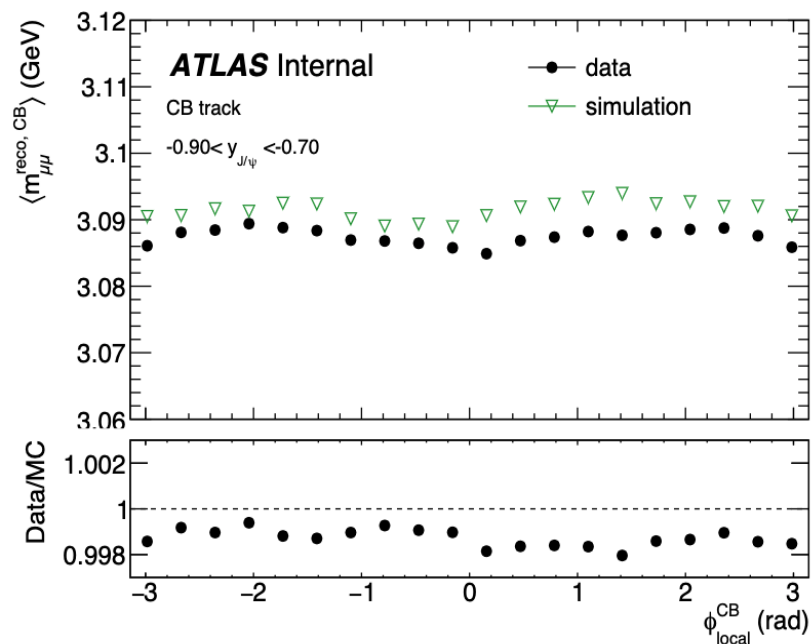
$$m_{\mu\mu}^2 \propto (1 - \cos \vartheta)$$



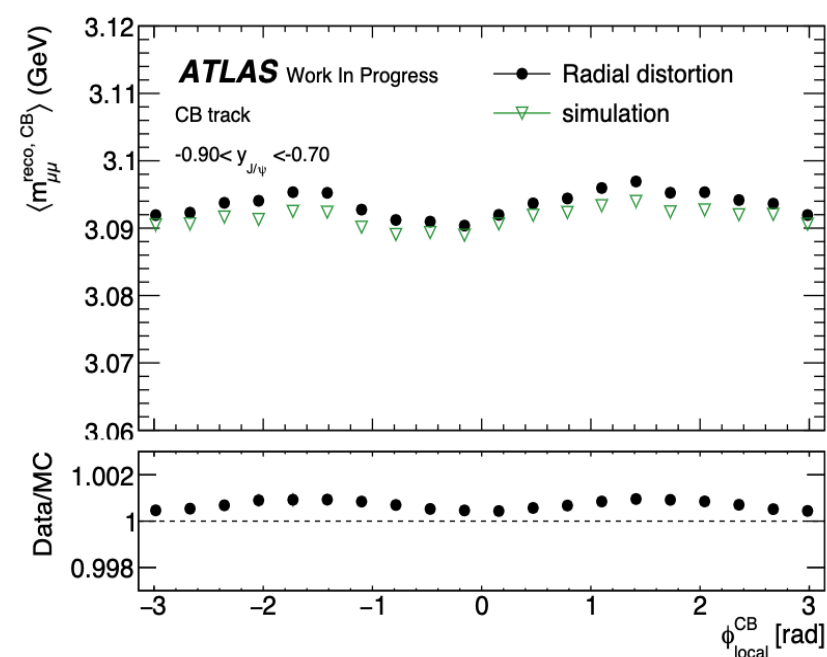
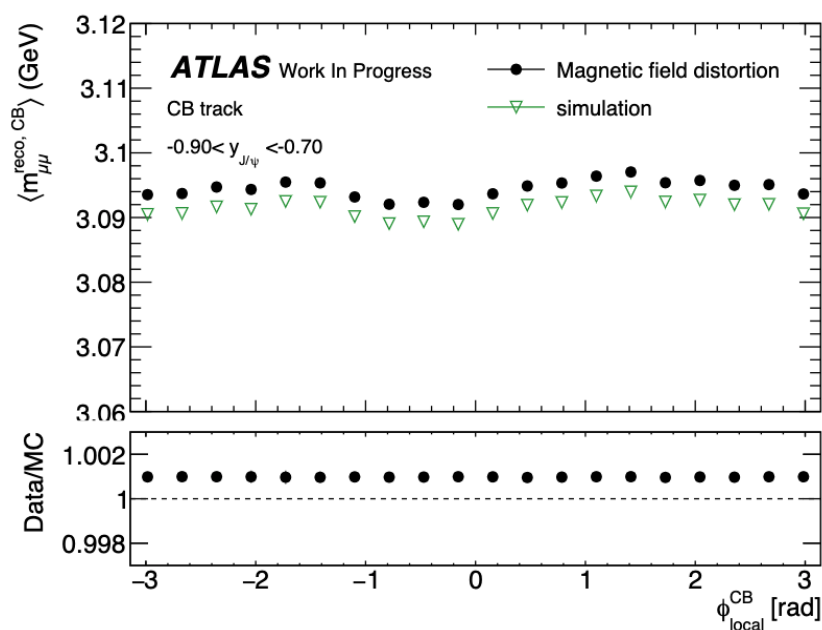
Similar behavior could appear if we expand the radial component ($x - y$ plane).

Data and simulation deformations

Data-to-simulation

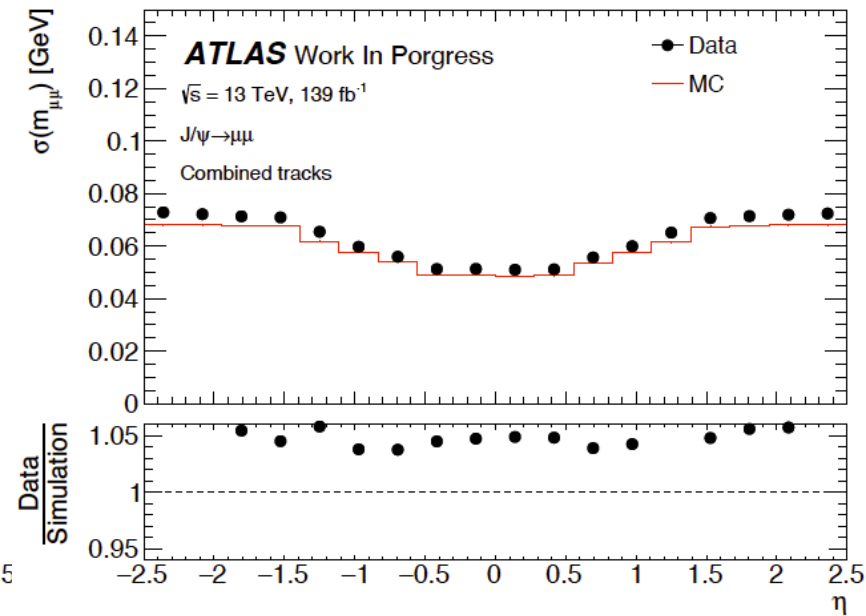
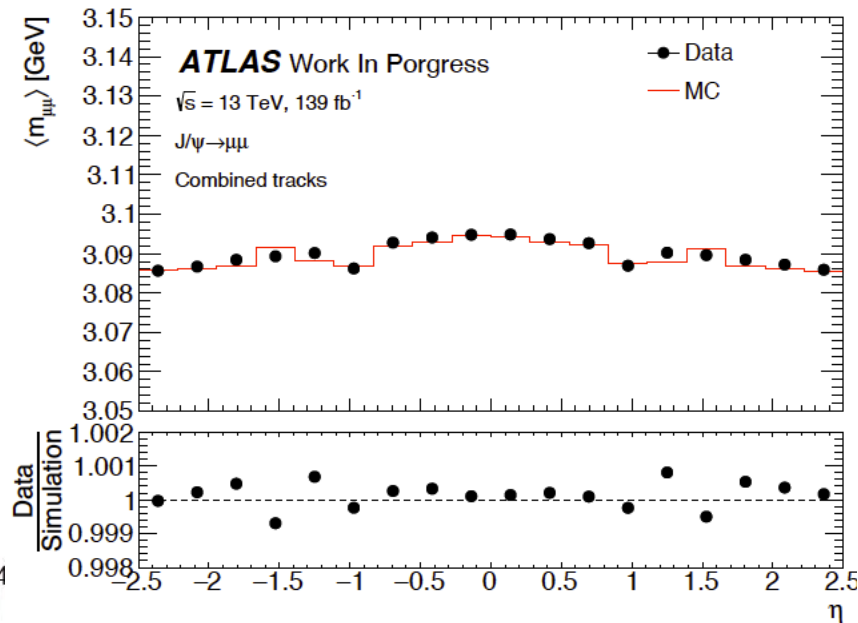
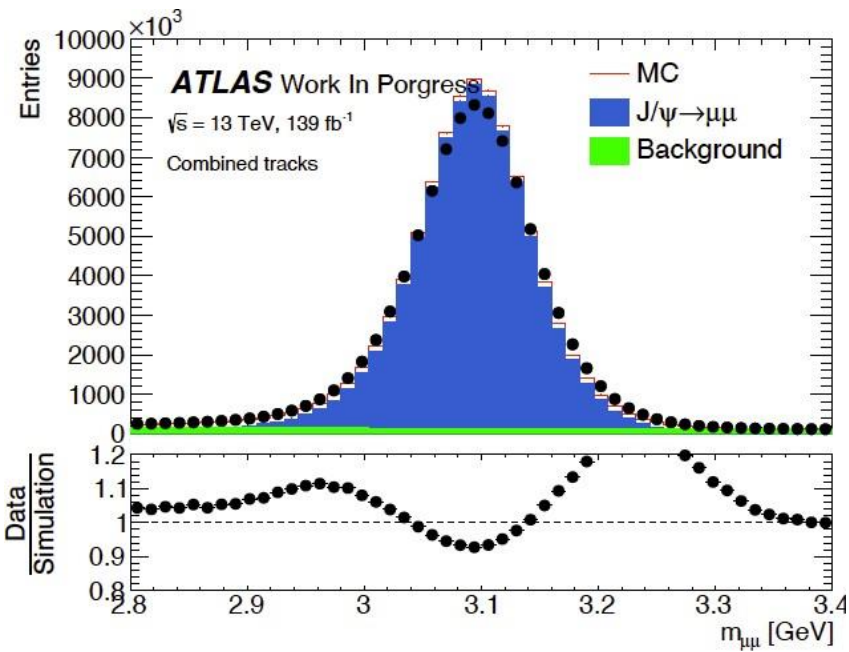


Model-to-simulation



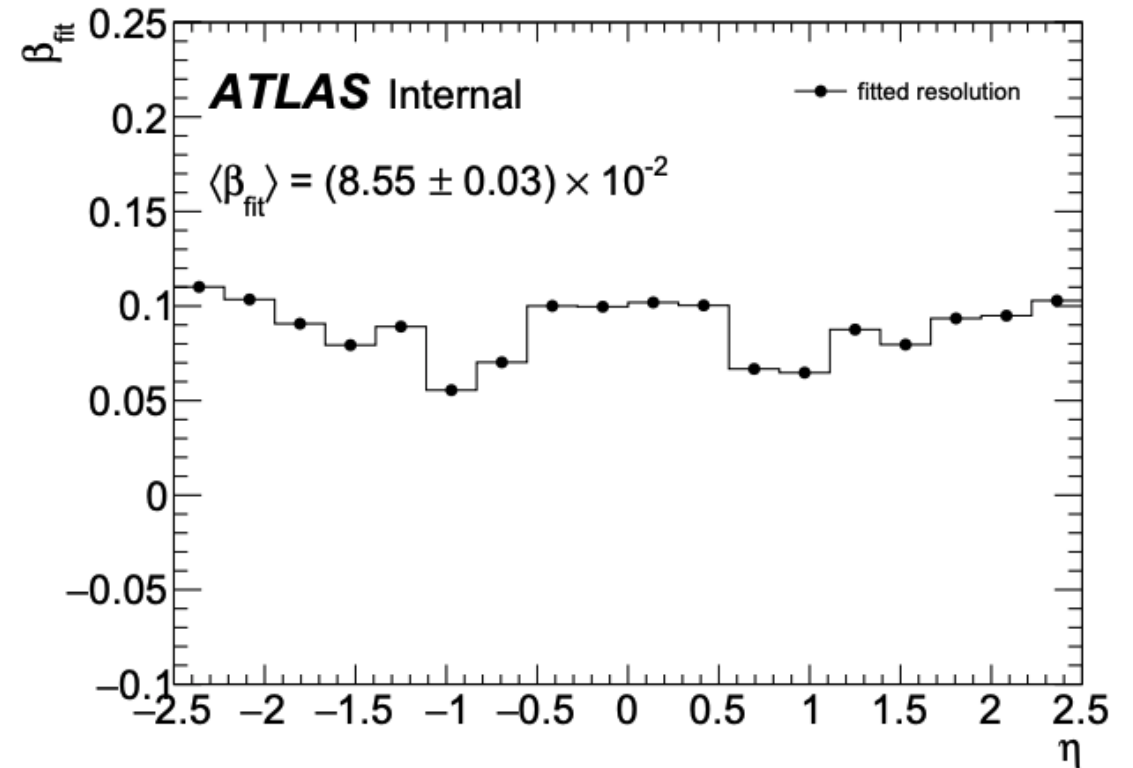
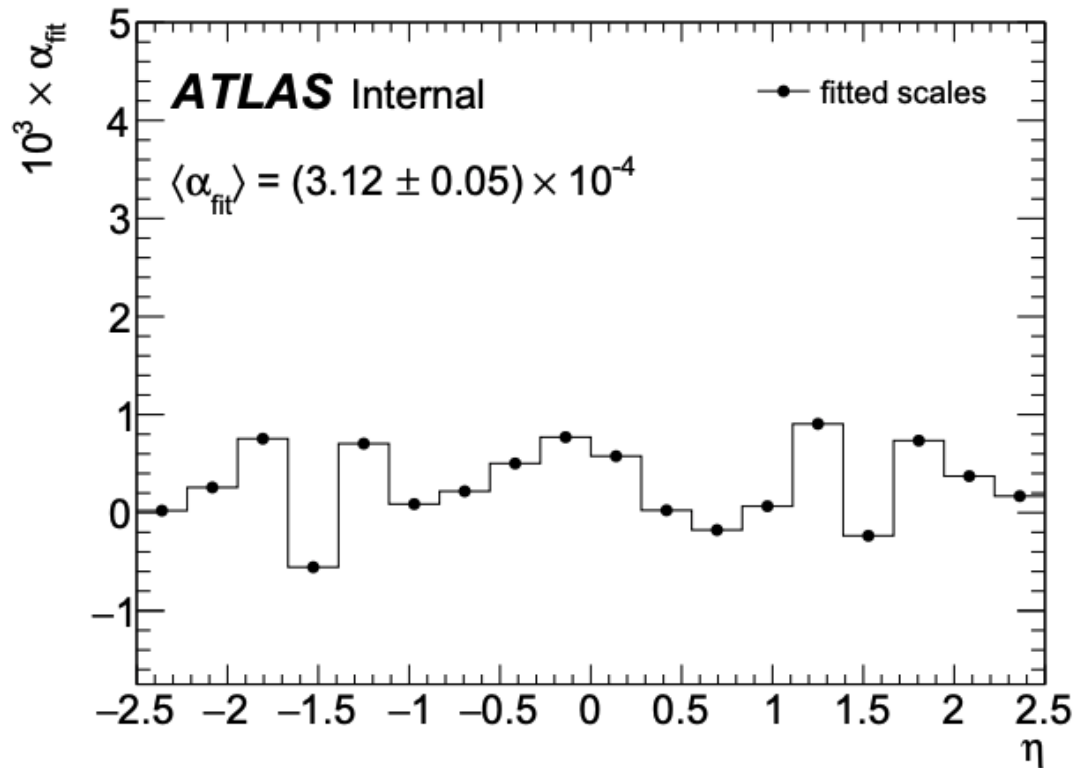
Correcting the ID deformations

- After correction, an improvement in the scale is obtained (with a small residual).
- An additional step is needed to improve the resolution and remove the residual in scale.



Scale and resolution maps

Scales are found in average $\langle \alpha_{fit} \rangle = (3.12 \pm 0.05) \times 10^{-4}$ while the resolution is about $\langle \beta_{fit} \rangle = (8.55 \pm 0.03) \times 10^{-2}$.



Kinematic categories and uncertainties

The fits are performed in 28 kinematic categories

Decay channel	$W \rightarrow e\nu$	$W \rightarrow \mu\nu$
Kinematic distributions	p_T^ℓ, m_T	p_T^ℓ, m_T
Charge categories	W^+, W^-	W^+, W^-
$ \eta_\ell $ categories	[0, 0.6], [0.6, 1.2], [1.8, 2.4]	[0, 0.8], [0.8, 1.4], [1.4, 2.0], [2.0, 2.4]

The following uncertainties are considered:

Experimental uncertainties:

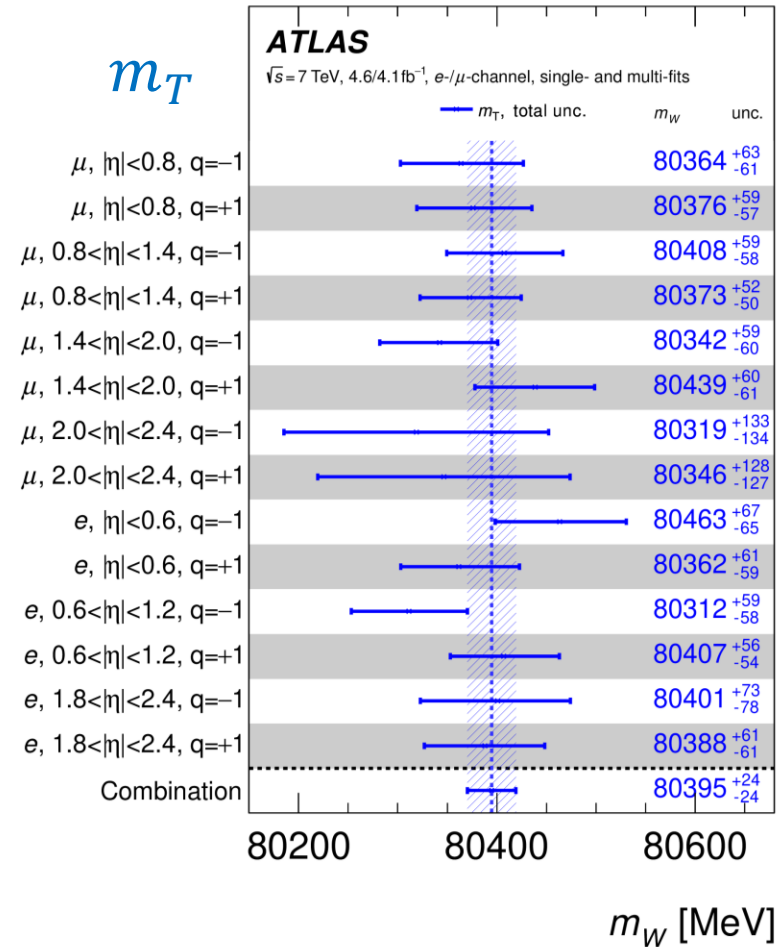
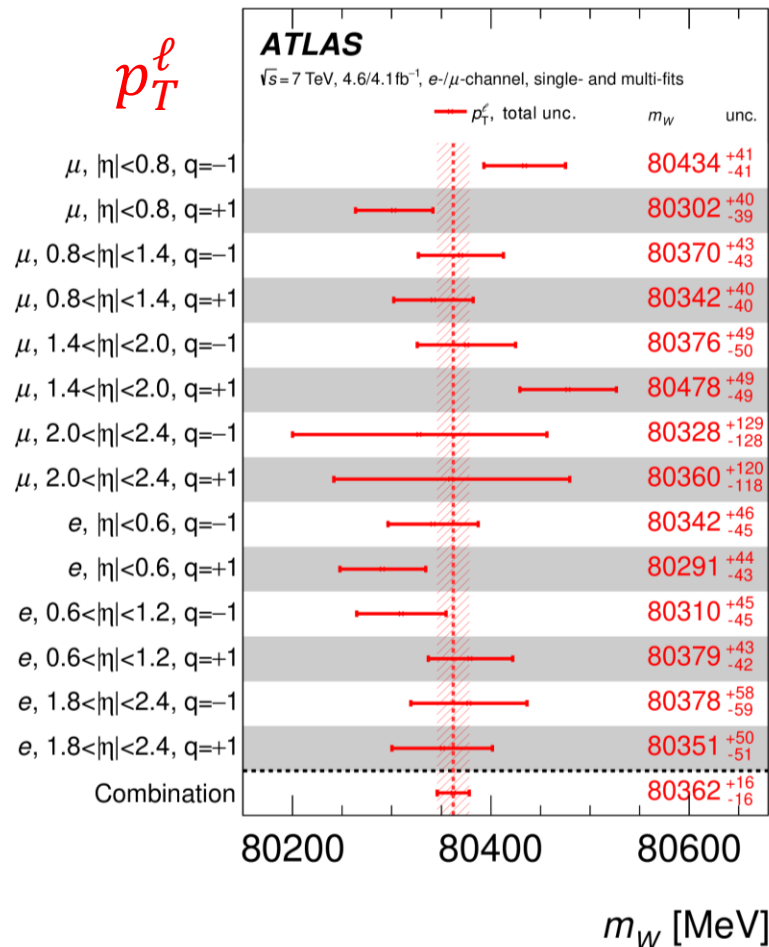
- Lepton calibration, efficiency, recoil calibration
- Luminosity, Multijet (MJ) background

Theoretical uncertainties:

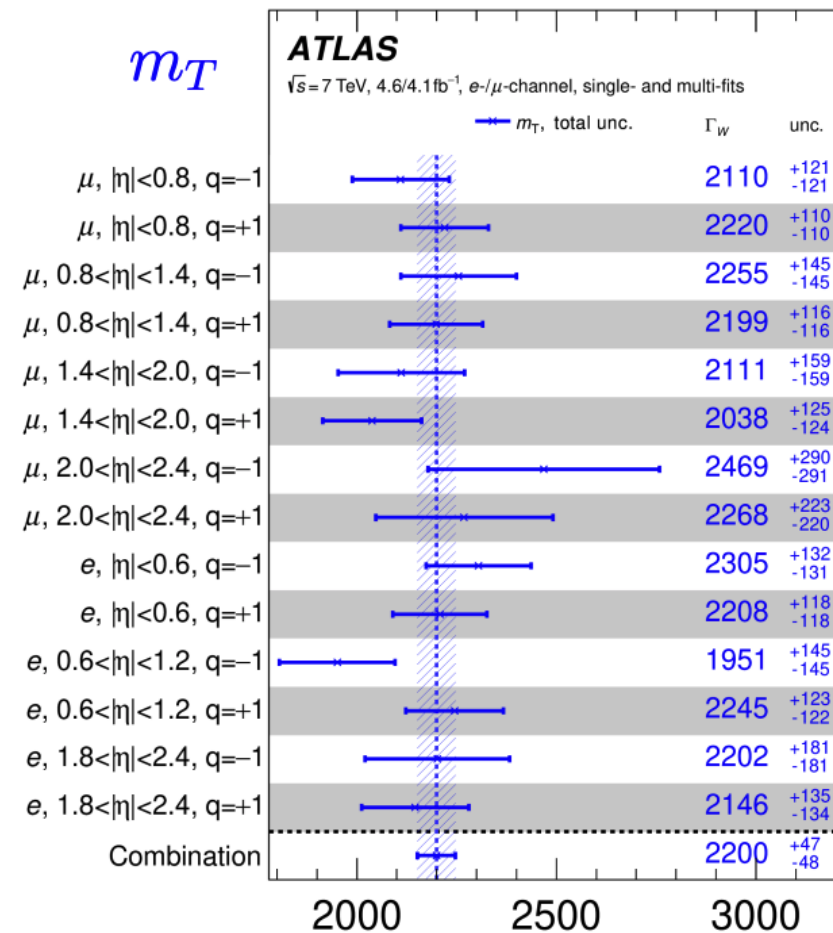
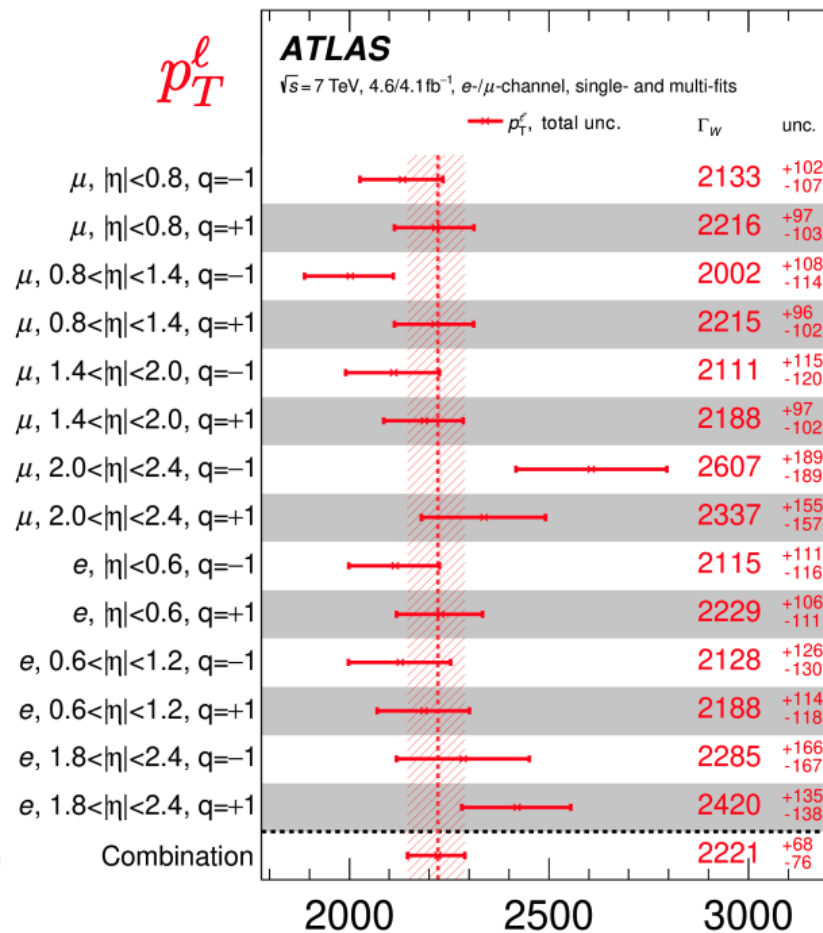
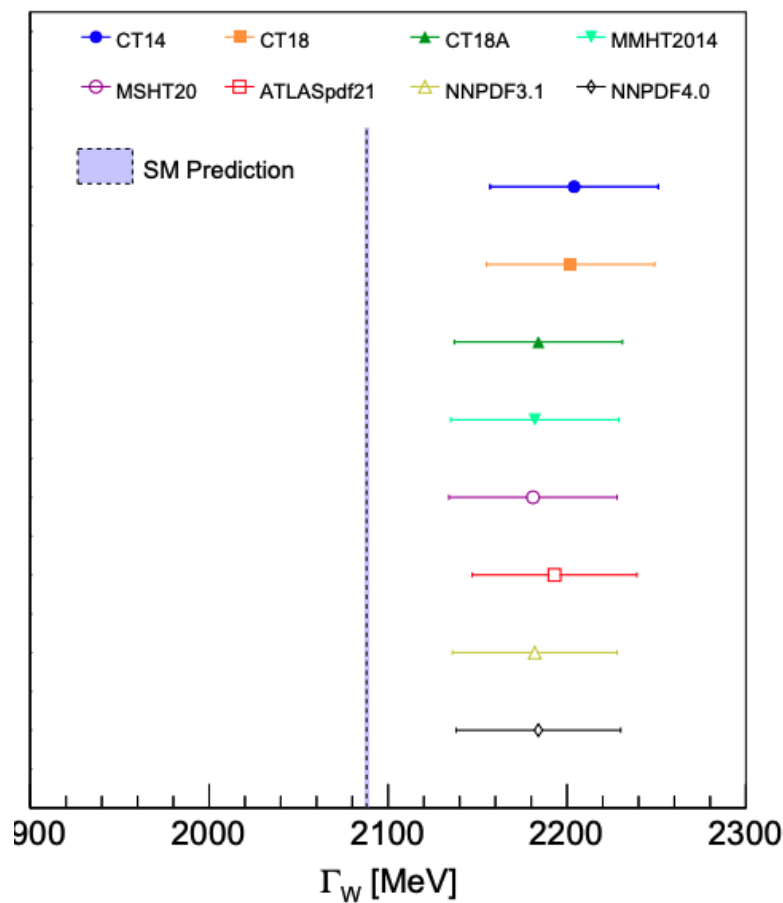
- p_T^W modelling
- Background cross-section uncertainties
- Parton distribution functions (PDFs)
- QCD predictions
- Electroweak corrections

m_W measurement at $\sqrt{s} = 7$ TeV

In each category, a separate fit for p_T^ℓ (left) and m_T (right) is performed, followed by a combined fit across all categories. Results show good compatibility.

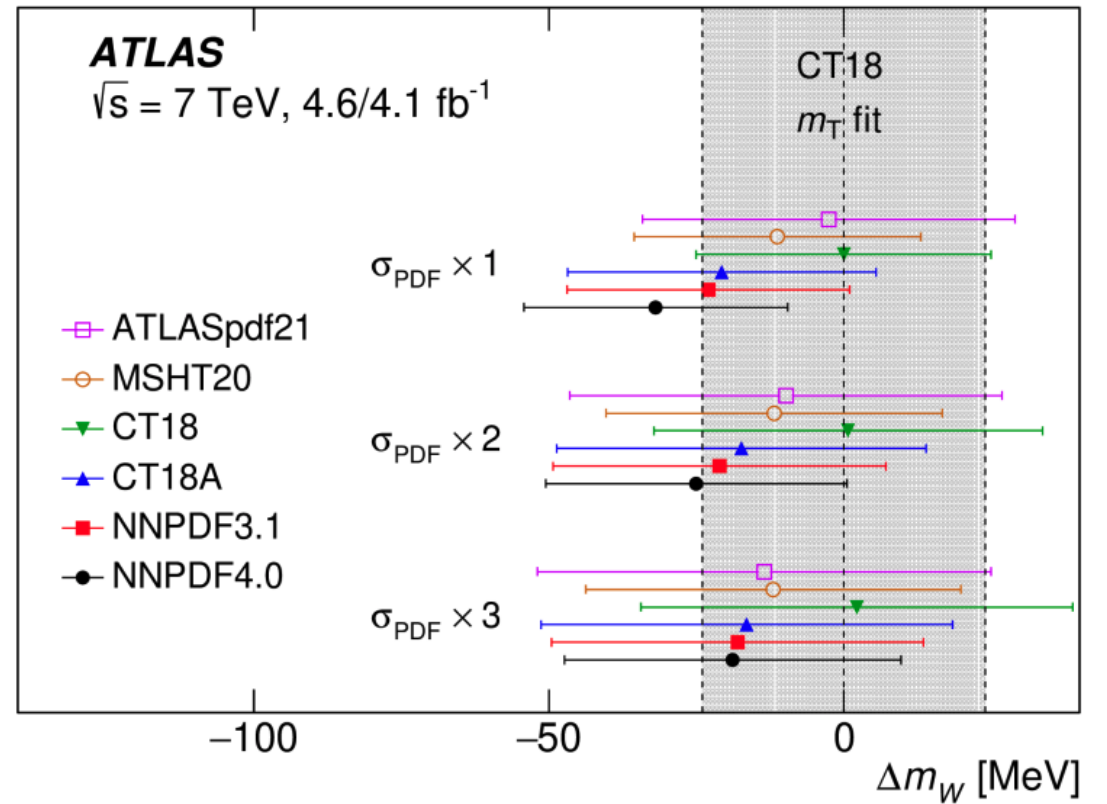
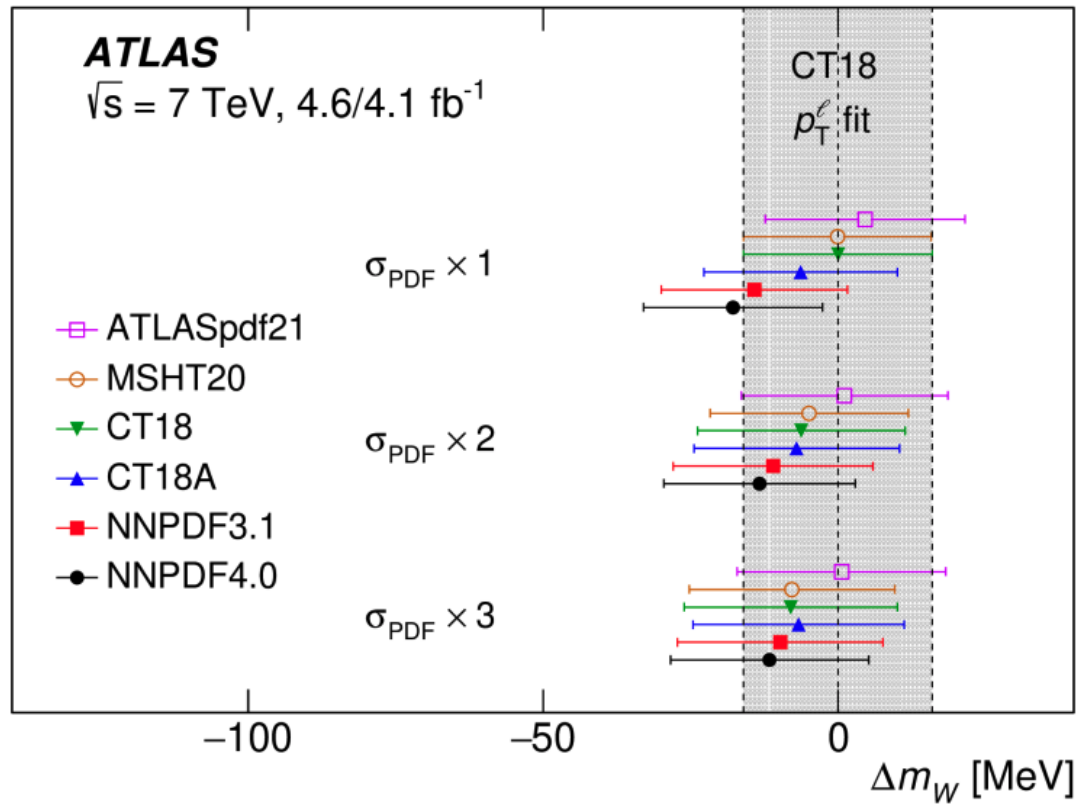


Γ_W category fits and PDF dependency



PDF dependency at $\sqrt{s} = 7$ TeV

Fits are performed for p_T^ℓ and m_T using different PDF sets to study the m_W dependency



m_W Nuisance parameters pulls

